Universidade de Aveiro
2019

Departamento de Ciências Médicas

Ana Carolina Fernandes Vieira de Castro

Nanopartículas de Óxido de Zinco sub-tóxicas modulam os níveis das proteínas PSD-95 e SHANK 3.

Sub-toxic Zinc Oxide Nanoparticles modulate PSD-95 and SHANK 3 protein levels.

Universidade de Aveiro
2019

Departamento de Ciências Médicas

Ana Carolina Fernandes Vieira de Castro

Sub-toxic Zinc Oxide Nanoparticles modulate PSD-95 and SHANK 3 protein levels.

Dissertação apresentada à Universidade de Aveiro para cumprimento dos requisitos necessários à obtenção do grau de Mestre em Biomedicina Molecular, realizada sob a orientação científica da Doutora Odete Cruz e Silva, Professora Associada com Agregação do Departamento de Ciências Médicas da Universidade de Aveiro, co-orientação da Doutora Maria de Lourdes Pereira, Professora Associada com Agregação do Departamento de Ciências Médicas da Universidade de Aveiro.

Esta dissertação contou com o apoio financeiro do Instituto de Biomedicina (iBiMED) - UID/BIM/04501/2013 e PTDC/DTP¬PIC/5587/2014, e Projeto CICECO – Aveiro Institute of Materials, FCT – UID/CTM/50011/2019.

DECLARAÇÃO DE DIREITOS DE AUTOR

Declaro por minha honra que a tese/dissertação que agora entrego à Universidade de Aveiro em suporte papel e em CD corresponde à versão final.

Nome: Ana Carolina Fernandes Vieira de Castro

Nº. do B. I.: 269434151 **Tel. /Telem.:** 919153854 **e-mail**: carolina.castro@ua.pt

Mestrado

Designação do mestrado: Biomedicina Molecular

Ano de conclusão: 12/12/2019

Título da dissertação: Sub-toxic zinc oxide nanoparticles modulate PSD-95 and SHANK 3 protein levels.

Orientadores: Doutora Odete Cruz e Silva e Doutora Maria de Lourdes Pereira

Dedico este trabalho aos meus avós, pais, irmãos e amigos por me ensinarem a nunca desistir e me apoiarem nesta jornada.

O júri

Presidente	Professor Doutora Daniela Maria Oliveira Gandra Ribeiro Investigadora Auxiliar do Departamento de Ciências Médicas, Universidade de Aveiro
Arguente	Professora Doutora Maria Paula Polónia Gonçalves Professor Associada do Departamento de Biologia, Universidade de Aveiro
Orientador	Professor Doutora Maria de Lourdes Pereira Professora Associado com Agregação do Departamento de Ciências Médicas, Universidade de Aveiro

Agradecimentos

Agradeço à professora Doutora Odete Cruz e Silva pela oportunidade de ter feito parte do seu grupo de investigação, pela orientação e por todo o carinho demonstrado ao longo destes dois anos do meu percurso no Mestrado de Biomedicina Molecular.

À professora Doutora Maria de Lourdes Pereira, pela co-orientação, pela dedicação, preocupação e cuidado durante este ano.

Ao André pela paciência, dedicação e pela disponibilidade que demonstrou no meu percurso no laboratório.

À Filipa, ao Daniel, à Idália e ao Pedro por me mostrarem que desistir nunca é uma opção, por tornarem este percurso uma grande brincadeira e por me ouvirem, a rir ou a chorar. Só alcançamos o mundo se nos rodearmos de pessoas que nos querem bem.

Ao Vasco, ao Bernardo, à Clara, à Sussu, à Adriana e à Maria. O tempo passa e a amizade verdadeira fica. E tive mais certeza que era verdadeira ao longo deste ano porque com um telefone, um café ou uma mensagem faziam tudo valer a pena mesmo quando achava ser impossível.

Aos meus pais, irmãos e avós por acreditarem e me proporcionarem os melhores anos da minha vida. Posso ter tudo e o maior sucesso, mas o alicerce são vocês. Aprendo convosco, diariamente, que a batalha da vida é dura, mas o segredo para a vencer é ter a única arma que nos torna invencíveis, uma família como vocês.

Palavras-chave Synaptic transmission, oxide zinc nanoparticles, neurodegenerative diseases, SH-SY5Y cells, SHANK 3, PSD-95, β-actin.

Resumo The effect of zinc on neuronal systems is growing interest in scientific research due to a possible role as a modulator of synaptic activity. Additionally, recent research points to the therapeutic potential of zinc oxide nanoparticles (ZnO NPs) on neuronal cells. These nanoparticles are excellent drug carriers to the brain because, besides having positive characteristics for the protection of cellular homeostasis, they are small, allowing them to pass the blood brain barrier and interact directly within these cells. In this sense, the present thesis explored the effect of sub-toxic ZnO NP concentrations on cell viability and ROS production in SH-SY5Y cells, as well as their impact on the expression levels of PSD-95, SHANK 3 and β-actin proteins. The results showed increases in PSD-95 and SHANK 3 protein expression without variations in β-actin expression after neuronal cell exposure to sub-toxic concentrations and at reduced exposure times to ZnO NPs. Future efforts should be implemented to investigate how this increase may reduce brain impairment associated with neurodegenerative diseases. However, the results here presented have clearly identified some of the synaptic molecular targets of ZnO NPs and that these NPs are worthwhile exploring for their therapeutic potential.

Keywords Transmissão sináptica, nanopartículas de óxido de zinco, doenças neurodegenerativas, células SH-SY5Y, SHANK 3, PSD-95, β-actina.

Abstract O efeito do zinco nos sistemas neuronais está a aumentar o seu interesse na pesquisa científica devido a um possível papel como modulador da atividade sináptica. Além disso, pesquisas recentes apontam para o potencial terapêutico de nanopartículas de óxido de zinco (ZnO NPs) em células neuronais. Essas nanopartículas são excelentes transportadoras de fármacos para o cérebro porque, além de terem características positivas para a proteção da homeostase celular, são pequenas, permitindo que elas ultrapassem a barreira hematoencefálica e interajam diretamente dentro dessas células. Nesse sentido, a presente tese explorou o efeito de concentrações sub-tóxicas de ZnO NPs na viabilidade celular e produção de ROS em células SH-SY5Y, bem como seu impacto nos níveis de expressão das proteínas PSD-95, SHANK 3 e β-actina. Os resultados mostraram aumentos na expressão das proteínas PSD-95 e SHANK 3, sem variações na expressão da β-actina após a exposição das células neuronais a concentrações sub-tóxicas e em tempos de exposição reduzidos aos ZnO NPs. Esforços futuros devem ser implementados para investigar como esse aumento pode reduzir o comprometimento cerebral associado a doenças neurodegenerativas. No entanto, os resultados aqui apresentados identificaram claramente alguns dos alvos moleculares sinápticos das ZnO NPs e que vale a pena explorar o seu potencial terapêutico.

Table of contents

List of figures

List of tables

Abbreviations

Aβ	β-amyloid
Abp1	Actin-binding protein 1
AD	Alzheimer's disease
AMPA	α-amino-3-hydroxy-5-methyl-4-isoxazole propionic acid
Ank	Multiple ankyrin repeats
APP	Amyloid precursor protein
BBB	Blood-brain barrier
BCA	Bicinchoninic acid
BSA	Bovine serum albumin
CaMKII	Calcium/calmodulin-dependent protein kinase II
CNS	Central nervous system
CortBP	Cortactin-binding protein
ER	Endoplasmic reticulum
EZS	Early Zn^{2+} signalling
GABA	γ-aminobutyric acid
GKAP	Guanylate kinase-associated protein
GSSG	Glutathione disulfide

HD	Huntington’s disease
HTT	Huntingtin gene
IP_3R	Triphosphate receptor
LB	Loading Buffer
LB NPs	Lipid-based NPs
LTP	Long-term potentiation
LZS	Later Zn^{2+} signalling
MAGUKs	Membrane-associated guanylate kinases
MAP/ERK	Extracellular signal-regulated kinase pathway
MAPK	Motigen-activated protein kinase
mGluR	Metabotropic glutamate receptors
mHTT	Mutant HTT protein
MTs	Metalloproteins
MTFs	Metal response element-binding transcription factor
MRE	Metal response element
NFTs	Neurofibrillary tangles
NMDA	N-methyl-D-aspartate
NPs	Nanoparticles
PDZ	Proline-rich domain
PKC	Protein kinase C
Pro	long proline-rich region
PSD	Post-synaptic density
PTPs	Protein tyrosine phosphatases
SAM	Sterile alpha motif

SEM	Scanning electron microscopy
SFs	Straight filaments
SH3	Src 3 domain
SSTRIP	Somatostatin receptor interacting protein
TFIIIA	Transcription factor IIIA
TMDs	Transmembrane domains
TP	Tyrosine phosphatases
VDCC	Voltage-gated calcium channels
ZFP	Zinc finger proteins
ZIPs	Zinc- and iron-like regulatory proteins
Zn	Zinc
ZnO	Zinc Oxide
ZnO NPs	Zinc Oxide Nanoparticles
ZnTs	Zinc transporters

1. Introduction

"A hundred times every day I remind myself that my inner and outer life are based on the labors of other men, living and dead, and that I must exert myself in order to give in the same measure as I have received and am still receiving."

Albert Einstein

1.1 Motivation

Nowadays, nanotechnology has been extensively used in several areas from commercial food applications to therapeutic strategies. Engineering of materials at the nanoscale level allow scientists to develop an efficient method for new discoveries with a possible high impact in industries and society. Due to recent evidences, nanomaterials can contribute to societal challenges that englobe sustainability, energy generation, conservation, storage and conversion with a surprising and lower-cost impact in healthcare. Several studies show that nanomaterials elicit toxicity in humans and this field turned scientists' attention to unravelling nanoparticles interactions with the nervous system. The human brain is extremely complex, presenting challenges in terms of treatment of many neurological diseases, conditioning the welfare and quality of life of patients. Therefore, this research is focused on applying a specific type of nanomaterials called nanoparticles (NPs) to neuronal cells. Previous studies have shown the ability of NPs to cross the blood-brain barrier thus providing alternative therapeutic strategies. Among the large number of existing nanoparticles, zinc oxide nanoparticles (ZnO NPs) have been studied in the central nervous system due to the action of zinc on synaptic transmission, thus they were used in this study to get pertinent information from a molecular level.

1.2 Thesis Structure

This thesis aims to understand the mode action of ZnO NPs at sub-toxicity concentrations in human SH-SY5Y cells. Therefore, it was essential, in the first phase, to get information on zinc, as well as its role in the proper functioning of the human organism, especially in the brain and neuronal system. A detailed introduction is presented that describes some aspects concerning to the impact of zinc on the human body, namely the zinc biochemistry as a metal, its functioning in the neuronal systems, its role in signalling and regulation of homeostasis and its interaction associated with neurodegenerative diseases.

NPs were also introduced including the characterization process and synthesis methods. Existing NPs groups were considered, to try to consolidate the possible effect of NPs in biomedical research and their use as a drug delivery mechanism to combat several diseases, particularly neurodegenerative diseases.

Then, methods used for ongoing research are described in accordance with the objectives defined in chapter 3. Accordingly, feasibility tests were first performed to understand the impact of NPs on neuronal cells as well as to compare their effect against free zinc. Having stablished conditions for application of ZnO NPs under sub-toxicity to SH-SY5Y cells, protein levels of specific proteins, PSD-95, SHANK 3 and β-actin were tested.

Results are presented in chapter 5, discussed in chapter 6 in order to draw working conclusions and define new future perspectives, as described in chapter 7.

2. State of the Art

> “The important thing is to not stop questioning. Curiosity has its own reason for existing.”
>
> **Albert Einstein**

2.1. Zinc impact in the human body

Numerous studies have contributing towards elucidating the role of zinc (Zn) in the human body. In living organisms, Zn was first recognized in *Aspergillus Niger* (Raulin J., 1869). Later, it was identified as an essential micronutrient for humans with several diseases (Halsted, 1961). Nowadays, Zn is considered the second most common trace element in living organisms (Kambe *et al.*, 2015). They have high impact on the human body at many levels, due to its function in protein and acid nucleic metabolism, stimulation of the activity of over 100 enzymes and its collaboration in the proper functioning of immune system (Kambe *et al.*, 2015).

2.1.1. Zinc biochemistry

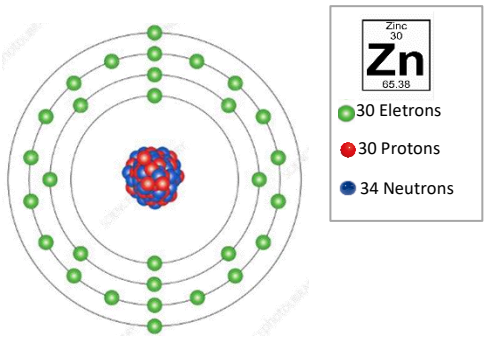

Figure 1 – Atomic composition of ^{64}Zn. Nucleus is composed by 30 protons **(red)** and 34 neutrons **(blue)** with electron configuration of 30 electrons **(green).** Adapted from (Science Photo Library).

Zn as a chemical element was described by *Andreas Sigismund Marggraf* in 1746 (Weeks, 1932). It is presented in the periodic table as a strong transition metal located in the twelfth group, side subgroup and fourth period with the symbol "Zn"; atomic number 30 and 65.4 atomic mass units **(Figure 1)**. This metal is an electron acceptor with the electron configuration of the atomic outer shell of $4s^2$. Zn does not participate in redox reactions because it has the orbital $3d^{10}$ filled so it does not change in the oxidation state that is +2. In the human body, Zn was detected as a divalent cation Zn (II) (Zn^{2+}), a neutral redox ion that exists as a total amount of about 2-3 g, where 0.1 % is present in plasma and 80 % in serum (Reyes, 1996; Takagishi, Hara and Fukada, 2017). In the latter case, Zn^{2+} binds to serum albumin and the remaining 20 % of Zn^{2+} is bounded to α2-macroglobulin (Reyes, 1996; King, Shames and Woodhouse, 2000).

The dynamic state of Zn has now been explored due to newly optimized zinc-imaging techniques. They include small fluorescent sensor molecules, molecules designed to sense zinc ions, laser ablation inductively coupled plasma mass spectrometry, X-ray fluorescence microscopy and secondary ion mass spectrometry (Qiao *et al.*, 2006; Fahrni, 2007; Z. Qin *et al.*, 2011; Huang and Lippard, 2012).

2.1.2. Zinc in biological systems

The role of Zn began to be explored in 1920/21 by *Rost* with the discovery of significant amounts of Zn in the human brain and this was later confirmed by *Bodansky* (Rost, 1920; Bodansky, 1921; Fallis, 2013). Zn has a reactive performance as a Lewis acid in biological reactions enabling it to acquire multiple physiological functions with key roles at structural, catalytic level and as a component of intracellular and extracellular signaling **(Table 1)** (Andreini, Bertini and Cavallaro, 2011).

Table 1 - Multiple functions of zinc as a component of biological processes (Andreini, Bertini and Cavallaro, 2011; S. V. Razin, V. V. Borunova, 2012; Kluska, Adamczyk and Krężel, 2018).

Structural component	Catalytic factor	Intracellular signaling mediator	Extracellular signaling mediator
→ **Component of zinc fingers** **C2H2-like finger -** classical zinc finger motif discovers in the eukaryotic transcription factor III A (TFIIIA) (Miller, Mclachlan and Klug, 1985); **Zinc ribbon –** present in many transcription factors, ribosomal proteins and in RanBP; **Treble clefs –** composed by RING, Arf-GAP, LIM, FYVE, PHD and MYND finger domains, nuclear receptor DNA-binding domain and GATA, PKC; **Gag necklaces –** composed by TAZ domain in transcriptional adaptor protein CBP/p300; → **Interprotein binding mediator -** Zinc hock motif; → **Crystallization of peptides –** insulin (Scott and Fisher, 1938).	→ **Enzyme cofactors of six main enzyme classes** **Oxidoreductase** - alcohol and sorbitol dehydrogenases; **Transferase** – 34% of zinc function in this class is catalytic; **Hydrolase** - carboxypeptidases, alkaline phosphatases, angiotensin-converting enzyme; **Lyase** - carbonic anhydrase, δ-aminolevulinic acid dehydratase **Isomerase** - phosphomannose isomerase; **Ligase** - 39% of zinc function in this class is catalytic.	→ **Secondary messenger functions** Inhibition of enzyme activity of caspases, protein tyrosine phosphatases and phosphodiesterases; Modulation of signaing pathways.	→ **Neuromodulating functions in the central nervous system** Activating zinc receptor (ZnR/GPR39); Reducing insulin secretion and suppressing hepatic insulin clearance;

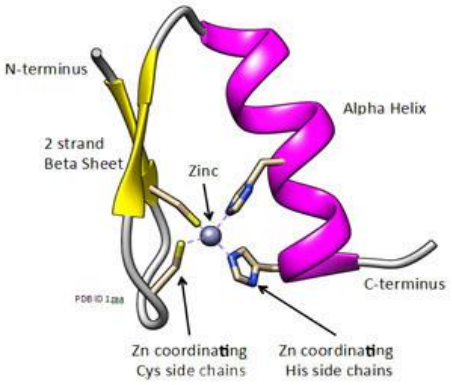

Figure 2 - Secondary structure of a single zinc finger protein domain. Structure is composed by two β strands and a single α-helix through which Zn^{2+} binding is stablished. Adapted from (*Genome Editing Proteins*, 2010).

In biological systems, Zn^{2+} ions are further classified as (a) Zn-binding-proteins and (b) labile Zn (Fukada and Kambe, 2014). Zn-binding proteins are molecular scaffolds that exist in micromolar concentrations that bind molecules to other proteins, lipids or nucleic acids (Krężel and Maret, 2006). Each Zn-binding protein contains two β-strands and a single alpha (α)-helix through which the protein motif is stabilized. Thus, two histidines of α-helix and two β-sheet cysteines bind simultaneously to Zn^{2+}, achieving this protein stabilization **(Figure 2)**. The configuration of different coordination numbers and various types of these protein binding residues allows them to adjust the affinities and functions of their binding sites (Ebert and Altman, 2008). Furthermore, the interaction of Zn^{2+} with proteins occurs in specific regions like the Zn-finger domains, LIM domains, PHD domains and RING finger domains that are small and compact. These domains have a finger-like dimensional aspect and are therefore referred to as Zn finger motifs (Kluska, Adamczyk and Krężel, 2018)**.** Binding of Zn finger motifs appear into more than 20 classes of structurally distinct modules (Klug, 2010; Krężel and Maret, 2016).

Based on the overall shape of the protein backbone and the folding domain, it is possible to classify Zn-binding proteins into key fold groups. These fold groups include ββα or Cys_2His_2, Gag knuckle, Treble clef, Zn ribbon, Zn2/Cys6 and Zn loops **(Table 1)** (Andreini, Bertini and Cavallaro, 2011; S. V. Razin, V. V. Borunova, 2012; Kluska, Adamczyk and Krężel, 2018)**.** Once bound to proteins by the β-sheet and α-helix layers, Zn^{2+} can induce a structural rearrangement, coordinating conserved positions of the polypeptide sequence. It can also establish a relationship with ligands such as nitrogen, oxygen and sulphur present in the histidine and cysteine residues or may also participate in the stabilization of

the quaternary structure (W. Maret, 2013). Of several connections included between the proteins and Zn fingers, each protein contains up to 36 Zn fingers (W. Maret, 2013). Depending of structural zinc sites, Zn may exhibit several functions at distinct level from transcription factors to ions transport. According to current literature and data mining for intramolecular zinc-binding sites, about 9 % of the proteins are Zn proteins in eukaryotes with the higher number in mammalian organisms (Andreini *et al.*, 2006). The human genome encodes about 10 % of Zn proteins corresponding to 3000 proteins that participate in Zn binding (Kochańczyk, Drozd and Krężel, 2015; Bafaro *et al.*, 2017).

In the case of labile Zn, which means "free" Zn^{2+} ions with absence of coordinating ligands, it exist in a range between the picomolar and nanomolar (Y. Qin *et al.*, 2011). The measurement of its concentration is extremely important in understanding the impact of Zn deregulation on human health.

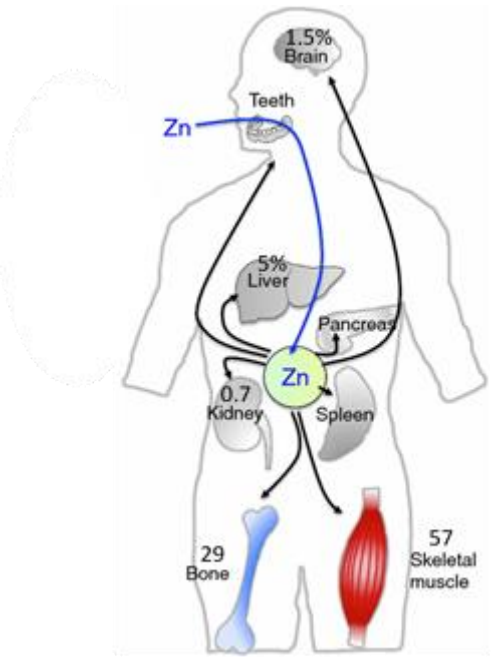

Figure 3 - Zn distribution and storage in the human body. The major proportion is in the bone and in the skeletal muscle. Relative percentages are indicated. Adapted from (T. Hara, T.Takeda, T.Takagishi, K. Fukue, T. Kambe, 2017)

Within the body **(Figure 3)**, Zn can be found throughout with approximate relative distributions of 0.1 % in hair, 0.1 % in blood plasma and the remainder in other tissues. Higher concentrations can be found in other tissues; 0.4 % in heart , 0.7 % in kidney, 1.5 % in the brain, 5 % in liver and in skin, 29 % in bone and 57 % in skeletal muscle (Jackson, 1989; Takagishi, Hara and Fukada, 2017).

2.1.3. Zinc in neuronal systems

In the human body, all actions, sensations, memories and emotions are driven by a network of highly conserved brain mechanisms. They work to ensure proper functioning and life. These mechanisms are developed by neuronal communication between neuronal cells (Purves D., 2015). They conduct electrical impulses and action potentials, away from the cell body or soma of presynaptic neuron to the postsynaptic neuron. The postsynaptic neuron receive excitatory and inhibitory outputs in the central nervous system (CNS) (Purves D., 2015).

In the presence of nervous stimulation, changes in the electrical potential of presynaptic neurons trigger the production and conservation of endogenous information. This information is in the form of chemical molecules, called neurotransmitters, inside of the synaptic vesicles. Subsequently, neurotransmitters are released into the synaptic cleft and bind to specific receptors on postsynaptic neurons. Postsynaptic neurons are composed by scaffold protein complexes that are assembled into an electron-dense region of the postsynaptic density (PSD). PSD serves as predetermined sites of postsynaptic activity responsible for trafficking, anchoring and clustering of glutamate receptors and adhesion molecules (Verpelli *et al.*, 2012). In addition, they link postsynaptic receptors with their downstream signaling proteins. Linkage allows them to regulate the dynamics of cytoskeletal structures. It also ensure synaptic transmission and long-term potentiation (LTP) in hippocampal synapses through excitatory and inhibitory outputs in the CNS (L. Squire et. al, 2008; E. Kim and M. Sheng, 2009).

Among the excitatory pathways of the CNS, the glutaminergic pathway is an important pathway. It uses glutamate as a neurotransmitter to influence synaptic plasticity (B. Pochwat, G. Nowak, 2015). Although the conditions that generate Zn^{2+} release are unknown, Zn^{2+} is known to participate in the glutaminergic pathway. It accumulates in synaptic vesicles. Zn^{2+} plays a significant role in synaptic transmission and act as an endogenous neuromodulator. It also is involved in nucleic acid metabolism and in brain microtubule growth. So, when synaptic vesicles merge, Zn^{2+} and glutamate are released from inside a presynaptic neuron into a postsynaptic neuron. Molecules enter in the postsynaptic terminals through specific ion channels. They include N-methyl-D-aspartate (NMDA) channel, γ-aminobutyric acid (GABA), voltage-gated calcium channels (VDCC) and

the α-amino-3-hydroxy-5-methyl-4-isoxazole propionic acid channel (AMPA) (Paoletti *et al.*, 2000; Frederickson, Koh and Bush, 2005; B. Pochwat, G.Nowak, 2015).

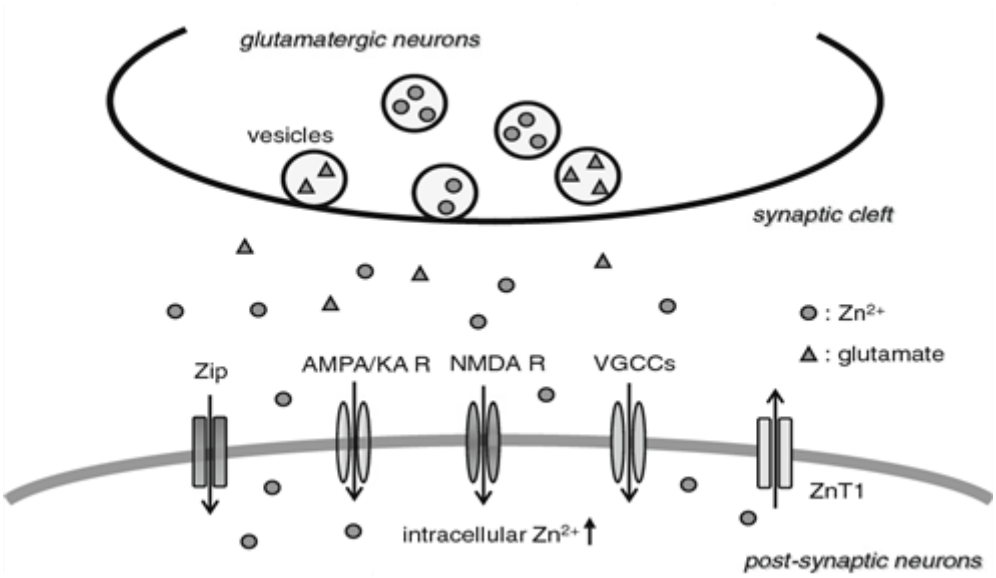

Figure 4 - Glutaminergic pathway of the CNS with accumulation of Zn^{2+} in synaptic vesicles of presynaptic neurons. Zn and glutamate are release into the cytoplasm of neighbouring cells through voltage-gated calcium channels (VDCC), calcium (Ca) ion-permeable AMPA/kainate channels and NMDAR on postsynaptic neurons for modulation of neurotransmission. Zn receptors are also depicted. Adapted from (B. Pochwat, G. Nowak, 2015).

All these channels may be potentiate or inhibit as a result of interaction with defined concentrations of Zn^{2+} **(Figure 4)** (Paoletti *et al.*, 2000; Frederickson, Koh and Bush, 2005; B.Pochwat, G. Nowak, 2015).

Under physiologic conditions, Zn^{2+} can potentiate AMPA and kainate receptor-mediated processes and inhibit glutamate uptake and GABA receptor function. They also may inhibit NMDA receptors and GABA transporters which promote or reduce excitation activity respectively (Molnár and Nadler, 2001; Blakemore and Trombley, 2004; E. Cohen-Kfir, W. Lee, S. Eskandari, 2005; D. Mott, 2008). Some authors estimate that during intense neuronal activity, released Zn^{2+} concentrations are approximately 10-100 µM. Nevertheless, under conditions of higher physiological stimulation, released Zn levels are less than 1 µM (Paoletti *et al.*, 2009).

In the postsynaptic terminal, specifically in PSD, Zn^{2+} plays an important role in several signal transduction pathways such as Calcium/calmodulin-dependent protein kinase II (CaMKII), Protein kinase C (PKC), and adenylyl cyclase (Canzoniero, Turetsky and Choi, 1999; Sindreu and Storm, 2011). Many processes are affected with Zn^{2+} interaction including plasticity induction, transcription modulation and protein synthesis (Sindreu and

Storm, 2011). Additionally, it can also influence the establishment of new functional excitatory synapses. In structural integrity, Zn^{2+} can be tightly bound to a specific domain of SHANKs, a family of proteins also known as somatostatin receptor interacting protein (SSTRIP), proline-rich synapse-associated protein 2 (ProSAP 2) or cortactin-binding protein (CortBP) with a molecular mass greater than 190 kDa. SHANKS are coded in different regions of the brain by three genes *SHANK 1, 2 AND 3.*

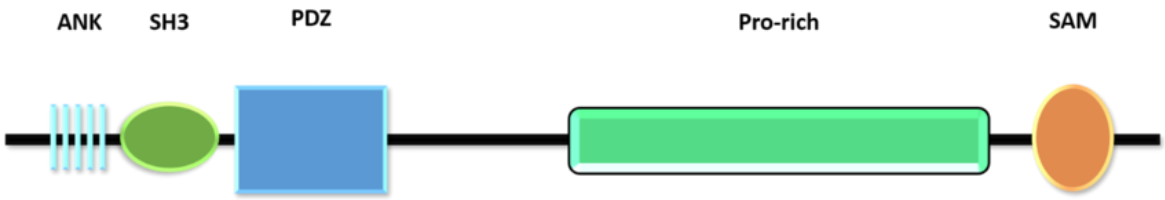

Figure 5 - Structural composition of SHANK 3. SHANK 3 is composed by ANK domain in N-terminal, a SH3 domains, a PDZ in full domain and a Pro and SAM domains in the C-terminal. Image from (ostales, 2015).

These genes are composed of multiple ankyrin repeats (Ank) , a src 3 domain (SH3), proline-rich domain (PDZ) in full domain, a long proline-rich region (Pro) and a sterile alpha motif (SAM) domain **(Figure 5)** (Boeckers *et al.*, 1999; M. Sheng and E. Kim, 2000; Sala *et al.*, 2001; Verpelli *et al.*, 2012). In the PSD, SHANKS represent an important category of scaffolding proteins. They are involved in aspects of synaptic development and function, modulating synaptogenesis and synapse maturation (Tao-Cheng *et al.*, 2016).

As noted by Tao-Cheng, members of SHANKS family are located in two pools at the PSD (Tao-Cheng *et al.*, 2015, 2016). One pool is near of the core and a second is in the distal layer of the PSD, where SHANK activity-induced accumulation preferentially occurs (Tao-Cheng *et al.*, 2015, 2016). SHANKS isoform domains are the synaptic directional signals through which these pools are in the postsynaptic density. These SHANKSs accumulation form two-dimensional matrices which regulate the initial formation and maintenance of nascent synapses. They also regulate maturation, stabilization and plasticity of mature excitatory synapses (Sala *et al.*, 2001). Strict regulation of SHANK 2 and 3 levels occurs in the SAM domain and depends of Zn^{2+}. They were shown to be two of the first proteins present in the development of PSDs that appear at the beginning of synapse formation (Grabrucker *et al.*, 2011). SHANK 3 is also capable of inducing functional dendritic spines in aspiny neurons. In the case of SHANK 1 dependence of Zn^{2+} does not occur (Baron, 2006). According to the literature, it is the last SHANK family member to appear at newly formed

synapses (Grabrucker *et al.*, 2011). SHANK 1 is needed to properly direct the synapse, rather than SHANK 2 and SHANK 3 (Grabrucker *et al.*, 2011). So, it appears to play an essential role in postsynaptic compartment morphology, maintaining spines and synapses located in the mouse hippocampal CA1 and CA3 regions, in the cerebral cortex and in the cerebellum (Roussignol *et al.*, 2005; Tao-Cheng *et al.*, 2016). These regions are both at Purkinje spines and in the molecular layer in PSDs of granule cells showing an acute activity-induced increase in PSD (Roussignol *et al.*, 2005; Tao-Cheng *et al.*, 2016).

In excitatory synapses, SHANK 3 has been shown to influence downstream effects such interaction with neuroligin-neurexins and ephrin-eph receptor (Meyer *et al.*, 2004; Futai *et al.*, 2007). This influence enables the signal to alter the transmission that occurs from PSD to the presynaptic site (Meyer *et al.*, 2004; Futai *et al.*, 2007). Consequently it stablish the synaptic contacts (Meyer *et al.*, 2004; Futai *et al.*, 2007). It can also influence several pathways in PSD.

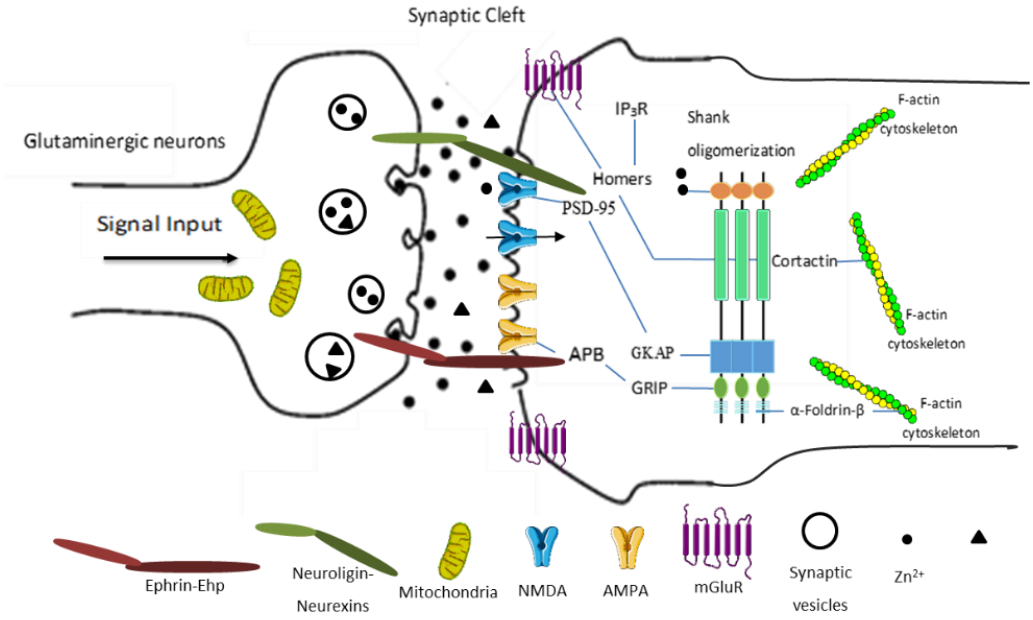

Figure 6 - Representation of pathways involved in SHANK modulation through binding-Zn^{2+}. Zn^{2+} binds to SHANKs promoting the oligomerization state of this Shank members. In this state, SHANK 1-3 bind to GKAP-PSD-95 complex acting as neuronal modulator for F-actin cytoskeleton and for neuronal transmission. SHANKs also bind to other proteins such Homers, Abp1, cortactin, α-foldrin-β and receptors such AMPAR.

Intracellularly, Zn supplementation or depletion was assumed to increase the density of the postsynaptic channels. Zn^{2+} enter in the postsynaptic compartment and bind to the SHANK 2 or 3 SAM domain by altering the oligomerization state of the SHANK members. After oligomerization, SHANK can stablish links with different pathways via its different

domains **(Figure 6)**. The SHANK 1-3 PDZ domain binds to the C-terminal Guanylate kinase-associated protein (GKAP) family members. Then, the N-terminal GKAP binds to the PSD-95 guanylate kinase (GK) domain and others membrane-associated guanylate kinases (MAGUKs) adjacent to the postsynaptic membrane. GKAP-PSD-95 interaction mediate the synaptic localization of SHANK in the PSD, closed to the nucleus (Naisbitt *et al.*, 1999). This recruitment of PSD-95 also interacts with neuroligin-neurexins, which recruits proteins from presynaptic release machinery for the function of releasing synaptic vesicles content (Roussignol *et al.*, 2005). Recruitment occur through retrograde modulation of new synapses and even dendritic spines formation (Roussignol *et al.*, 2005). SHANK-GKAP-PSD-95 complex formation can bind to NMDA receptors at postsynaptic sites, which promote neuronal synthesis of the nitric oxide and a GTPase Ras activating protein (Romorini *et al.*, 2004; Petralia, Al-Hallaq and Wenthold, 2008).

Although GKAP has been a critical determinant of SHANK synaptic localization, SHANK is not required for PSD-95/GKAP segmentation in synapses (Craven and Bredt, 1998). SHANK 1 and 3 may also bind to Homers to influence and organize other proteins, including Densin-180, dynamin-2, and actin regulatory elements such actin-binding protein 1 (Abp1) and cortactin (Verpelli *et al.*, 2012; Tao-Cheng *et al.*, 2015; Arons *et al.*, 2016). Homers´ binding also influences 1/5 metabotropic glutamate receptors (mGluR 1/5) clusters and interacts with the inositol triphosphate receptor (IP_3R). Thereby, they improve the relationship between PSD-95 and Homer complexes (Sala *et al.*, 2005). Recruitment of SHANK-binding proteins such Abp1 or cortactin into the distal layer in response to Zn-dependent synaptic activity can improve acute actin cytoskeleton regulation (Hering and Sheng, 2003; Qualmann *et al.*, 2004; Grabrucker *et al.*, 2009; Tao-Cheng *et al.*, 2015). They bind tightly to the cytoskeleton and C-terminal of the Pro region of SHANK 2 and 3, modifying morphology and enlargement of actin-based spines (Hering and Sheng, 2003; Qualmann *et al.*, 2004; Grabrucker *et al.*, 2009; Tao-Cheng *et al.*, 2015). In the case of IRSp53, it establishes the relationship between SHANK family complexes and insulin-dependent remodelling in PSD (Soltau *et al.*, 2004).

Finally, SHANK can also interact with AMPAR by binding to GRIP, forming a complex with ABP-activating AMPAR subunits. It also promote the functionalization of the Ephrin-Ehp receptor complex (Verpelli *et al.*, 2012).

2.1.4. Zinc signaling

Communication between cells is a complex process that allows cells to govern and coordinate cellular activities and functions that involves Zn^{2+}. Zn^{2+} can act as a ligand of specific receptors expressed on the cell membrane of target cells (Fukada and Kambe, 2014). Intracellular Zn^{2+} may participate in early or later cell signaling events that occur after extracellular stimulation. They were referred as early Zn^{2+} signaling (EZS) or later Zn^{2+} signaling (LZS) respectively. These events are distinguished by the time that it takes to cause changes in carrier expression (Fukada *et al.*, 2011). Zn^{2+} release occurs from Zn^{2+} stores such as endoplasmic reticulum (ER) or mitochondria, after direct application of extracellular stimuli (Fukada *et al.*, 2011).

Involvement of Zn^{2+} in signaling events is promoted by many specific transporters which are proteins necessary for the transport, orientation, release and regulation of cytosolic Zn^{2+} concentrations into the cells (Cousins and Liuzzi, 2006). Zn^{2+} can influence the expression of these transport proteins, however, this influence is regulated by metal response element-binding transcription factors (MTFs). In the presence of Zn^{2+}, MTF-1 is translocated to the nucleus, where interacts with metal response element (MRE) sequences presents in the Zn-regulated genes promoters (R. J. Cousins and Juan P. Liuzzi, 2006; Kimura and Kambe, 2016).

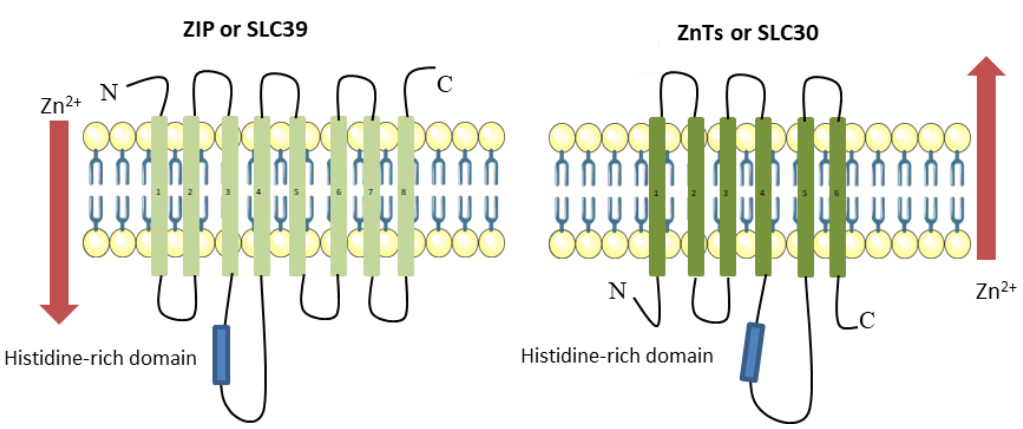

Figure 7 - Zn^{2+} transporters modulation (ZIPs and ZnTs). Transporters can exist in two ways, SCL39/ ZIP or SCL30/ ZnT. They are distinguished by Zn^{2+} mode of transport, performed either directly (ZIPs) or via synaptic channels (ZnTs). Adapted from (Eide, 2006).

Transporters can be distinguished into two known families, SLC39 or zinc- and iron-like regulatory proteins (ZIPs) and SLC30 or zinc transporters (ZnTs) (R. J. Cousins and J. P. Liuzzi, 2006). This two families (ZIPs and ZnTs) are distinct in the way of transport modulation (Frederickson, Koh and Bush, 2005). ZIPs carry a direct transport of Zn^{2+} uptake, while ZnTs can only modulate transport indirectly through synaptic channels (Frederickson, Koh and Bush, 2005). They also have predicted transmembrane domains (TMDs) with different orientations of N- and C-terminals. They still have a large histidine-rich domain with a distinct location on these transporters, between TMD-3 and TMD-5 respectively **(Figure 7)** (Frederickson, Koh and Bush, 2005).

ZnTs comprise 10 family members, ZnT1-ZnT10 **(Figure 8, Supplementary table 1)**, derived and preserved in different subcellular locations (Segal *et al.*, 2004). ZnTs bind to metal ions through the histidine region (Liuzzi and Cousins, 2004). They are associated with cellular Zn^{2+} efflux and transport from cytosol to extracellular space or intracellular compartments decreasing Zn^{2+} concentration in cytosol (R. J. Cousins and J. P. Liuzzi, 2006; Kimura and Kambe, 2016). ZIPs comprise 14 members derived and preserved in different subcellular locations **(Figure 8, Supplementary table 1)** (Liuzzi and Cousins, 2004). ZIPs function is transport Zn^{2+} to the cytosol of neurons and glia from the extracellular space or from intracellular compartments. These mechanisms increase the cytosolic Zn^{2+} concentration.

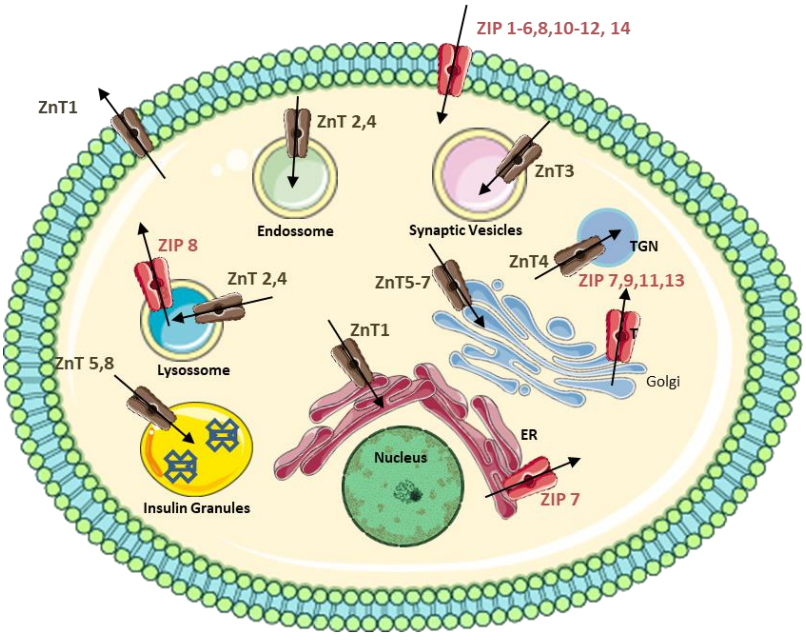

Figure 8 - Zn transporters distribution in mammalian cells. ZnTs are responsible for transport from cytosol into cells and ZIPs realize transport Adapted from (Kambe, Tsuji and Fukue, 2014).

The evidence that Zn^{2+} is an important signaling molecule, has fueled research in this area. The literature reports an interchangeable Zn^{2+} in discrete brain areas, restricted to the telencephalic regions (Frederickson, 1989). These regions are found in the hippocampus, cortex, striatum and tonsils, where, Zn^{2+} function as the first messenger in the regulation of synaptic transmission and plasticity (Frederickson, 1989). Zn also can act as second messengers of extracellular signals such cytokines or growth factor (Fukada and Kambe, 2014). It is capable of transducing the extracellular stimuli into intracellular signaling events, impacting the major signaling cascades involving Zn^{2+} (Yamasaki, 2007). Studies made by the application of an extracellular stimulus in mast cells revelead a change in Zn^{2+} concentration resultant from its release into the mast cell cytosol that inhibited the protein tyrosine phosphatases (PTP) activity, protein involved in signaling cascades capable of control cell adhesion and motility (Yamasaki, 2007).

Zn^{2+} can also influence other proteins and many enzymes involved in cell signalling including tyrosine phosphatases (TPs), phosphodiesterases, calcineurin, caspases and kinases such mitogen-activated protein kinase (MAPK), protein kinase C (PKC) and other many proteins (D. L. BrautiganS, Bornstein and B. Gallis, 1981; Hansson, 1996; V.v. Bülow, 2005; Aydemir *et al.*, 2009).

The regulatory and driving force of transporters and Zn^{2+} sensor molecules is crucial for the correct function of Zn^{2+} binding proteins in signaling pathways (R. J. Cousins and J. P. Liuzzi, 2006; Kimura and Kambe, 2016).

2.1.5. Zinc homeostasis

Maintaining systemic and cellular zinc homeostasis in mammals is crucial to the proper functioning of the human body.

Mobilization of Zn^{2+} require more than 30 proteins linked to a Zn^{2+}-sensing protein, metallothionein's (MTs). MTs are small, cysteine-rich proteins that have four isoforms, MT_{1-4} (Shabb, Muhonen and Mehus, 2017). MTs provide protection against oxidative stress and it can "buffer" against toxic heavy metals. It also can act as metallochaperones in controlling the storage and release of intracellular Zn^{2+}(Feng *et al.*, 2005; Maret, 2011;

Bafaro *et al.*, 2017). This control occurs by donating or accepting metals to metal-containing enzymes and transcription factors (Feng *et al.*, 2005; Maret, 2011; Bafaro *et al.*, 2017). Thus avoid possible zinc scavenging by non-specific proteins or other molecules (Feng *et al.*, 2005; Maret, 2011; Bafaro *et al.*, 2017). Because of the oxidoreductive property of MTs, the reduction potential of MT remains sufficiently low. Thus, specific oxidants such as disulphides and selenium compounds can oxidize cysteine sulphur ligands of MT reduction concomitantly. In the presence of a stimulus, Zn^{2+} concentrations increase, and MT interacts with glutathione disulphide (GSSG) to release Zn^{2+} (Krężel, Hao and Maret, 2007; Bell and Vallee, 2009). Release of Zn^{2+} occurs when the rate-limiting step of zinc-linked thiolates accessible to the solvent in each domain participates in a thiol / disulphide exchange. (Krężel, Hao and Maret, 2007; Bell and Vallee, 2009). In the process, GSSG causes clusters collapsing and oxidation of sulphur donors of one between the seven atoms of Zn^{2+} that MTs coordinate of each time (Krężel, Hao and Maret, 2007; Bell and Vallee, 2009). This cytosolic Zn^{2+} pool portion bounded to MTs was reported as existing in a total of 5-15 % (P. Coyle, J. C. Philcoxa, L. C. Careya, 2002).

Regulation of MT biosynthesis by metals has been considered as a biological necessity to maintain homeostatic concentrations of essential and non-essential metal ions. In cells, according to records, distribution of Zn^{2+} is made in the plasma and organelle membranes (10 %), in the cytoplasm (50 %) and in the nucleus (30-40 %) (Thiers and Vallee, 1957). Nuclear Zn is tightly bound to proteins while free or transiently Zn is found in the ER, Golgi apparatus and mitochondria (Lu *et al.*, 2016). Compartmentalization of Zn in different forms allows cells to regulate cellular functions and cooperate with transporters proteins to maintain Zn homeostasis.

2.1.6. Zinc signal in neurodegenerative diseases

Although Zn^{2+} plays a positive role in the human body, when the homeostasis of this ion change severe acute and chronic pathologies can be developed that condition human life. The excess of Zn^{2+} influx into neurons has been found in traumatic brain injury, stroke and epilepsy, behind influx deficiency, which leads to an increased risk for developing neurological disorders. Among the numerous pathologies associated with Zn^{2+}, neurodegenerative diseases stand out due to the lack of knowledge on the subject.

Neurodegenerative diseases involving Zn^{2+} dysfunctions include Alzheimer's disease (AD), amyotrophic lateral sclerosis, Parkinson's disease and Huntington's disease (HD) (V.Kumar, A. Kumar,S. K. Singh, S. Kumar *et al.*, 2016; Portbury and Adlard, 2017). AD and HD have characteristics in which the present work can constitute a promisor influence for their improvement aspects.

2.1.6.1. Alzheimer´s disease

Alzheimer's disease (AD) currently affects approximately 36 million people worldwide, with an estimated prevalence of over 115 million by 2050 (Gregori, Masserini and Mancini, 2015). Two pathologic features are associated with this form of dementia; extracellular senile plaques (SPs) and intracellular neurofibrillary tangles (NFTs), followed by neuronal loss in AD sensitivity brain regions (associative cortex, hippocampus and limbic nuclei). Characteristic clinical features include short-term memory loss, orientation and learning (Smith, 1998; Bohic *et al.*, 2011). The extracellular SPs are formed through deposits accumulating amyloid-β (Aβ) polypeptides resultanting from proteolysis of the amyloid precursor protein (APP) by an amyloidogenic pathway mediated by two membrane-bound endoprotease activities, β-secretase and γ-secretase (Crews and Masliah, 2010). NFTs are a product of tau phosphorylation that implies an inability to bind microtubules and instead polymerizes with other tau molecules, forming straight filaments (SFs) that subsequently form paired helical filaments (PHF); both constituents of NFTs (Mi and Johnson, 2006). In this condition, Zn^{2+} may increase with age in some regions of the brain or decreased in other regions, which makes the proportional relationship with AD difficult. At concentrations above 300 nM, Zn^{2+} may precipitate Aβ promoting aggregation and consecutive formation of senile plaques that destroy the neuronal parenchyma affecting cell exchange homeostasis. It can also enhance plaque number and size through dietary Zn^{2+} modulation. Micromolar Zn^{2+} concentrations have also been observed to regulate tau protein phosphorylation through the extracellular signal-regulated kinase pathway (MAP/ERK), contributing to the aggregation of human tau fragments, the formation of NFTs and mediation of tau toxicity through Zn^{2+} binding (Bohic *et al.*, 2011).

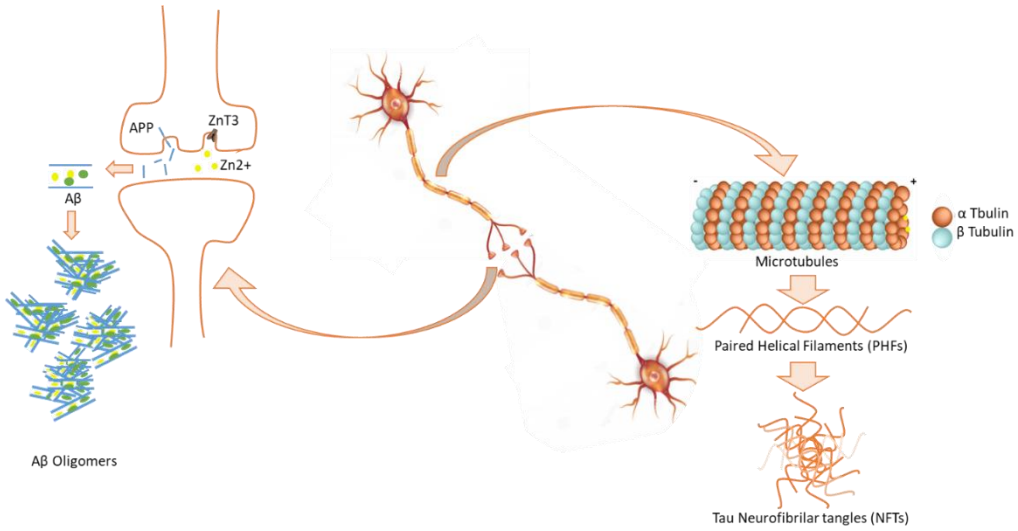

Figure 9 - Zn^{2+} interaction with molecular mechanism of AD. Aβ deposition and Tau formation can be developed through the Zn^{2+} binding with Aβ polypeptides and α, β tubulin respectively, producing Aβ oligomers and NFTs that characterize AD.

In low concentrations Zn^{2+} can be protective **(Figure 9)** (Bush and Tanzi, 2002; Lee *et al.*, 2002; Hynd, Scott and Dodd, 2004; Stoltenberg *et al.*, 2007). All this evidence supports the hypothesis that deregulated Zn^{2+} homeostasis can be involved in the pathophysiology of AD.

2.1.6.1. Huntington's disease

Huntington's disease (HD) is an inherited neurodegenerative disease caused by a mutation in one of the huntingtins (HTT) gene alleles. This mutation creates only a functional or healthy copy of HTT in the cell, which produces the mutant HTT protein (mHTT). mHTT leads to profound neuronal loss and progressive deterioration of HD associated motor, psychiatric and cognitive abilities.

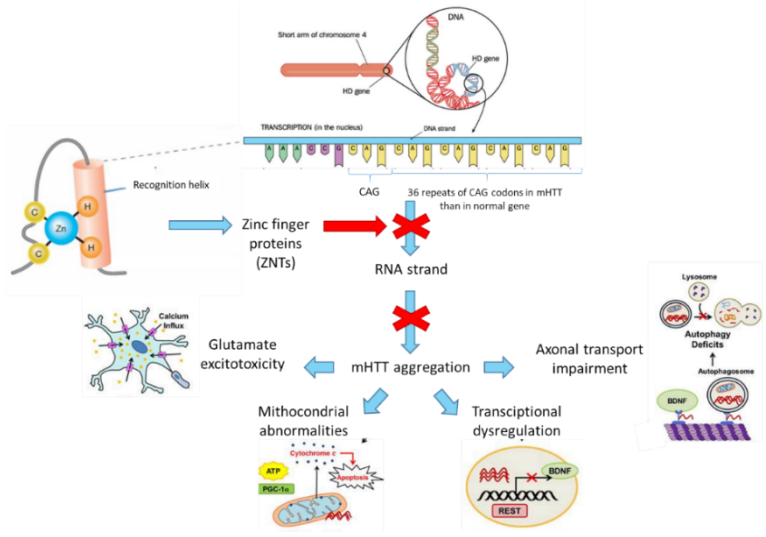

Figure 10 - Zn^{2+} interaction with molecular mechanism of HD. Adapted image from (Scheuing *et al.*, 2014, Huang, Chen and Zhang, 2016).

The relationship between HD and Zn^{2+} occurs because ZFP proteins can recognize and bind to specific DNA sequences of that gene, preventing the expression of mHTT containing these repeats and consequently reducing the production of HTT **(Figure 10)** (Garriga-Canuta *et al.*, 2012; Therapeutics, 2019)

2.2. Nanoparticles

A reference point for nanotechnology is the lecture “There’s Plenty of Room at the Bottom”. It described a process from which it might be possible to manipulate individual atoms and molecules, with resources to a set of precise tools, in order to construct and operate other proportionally smaller materials of various types at nanoscale levels (Wu and Yu, 2017). These materials, called nanoparticles (NPs), are a wide class that includes particulate substances that have one dimension less than 100 nm at least. Later, the “Engines of Creation: The Coming Era of Nanotechnology” supported and confirmed the Feynman´s idea and proposed a nanoscale "assembler" that would be able to construct a copy of himself and other items of arbitrary complexity controlling by a computer (K. Eric Drexler., 2006).

2.2.1. Characterization of nanoparticles

NPs has been revealed to play an important role in physicochemical properties of a substance due to their small size whereby they have attracted interest in scientific research from biotechnology, biosensors, microfluidics, drug delivery, and microarray tests to tissue engineering like energy storage, magnetic fluids or catalysis (F. A. Khan, D. Almohazey, M. Alomari, 2018).

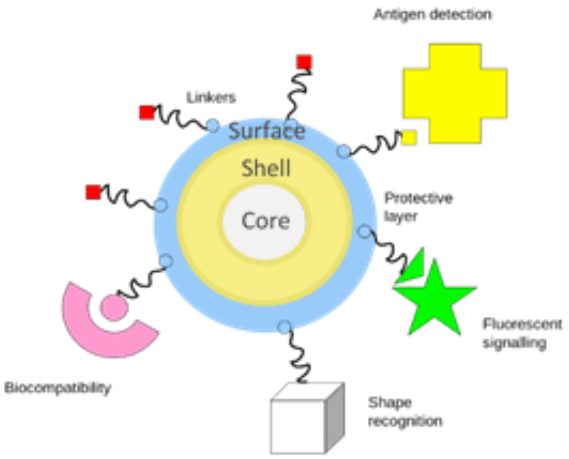

Figure 11 - Composition and multifunctionalities of nanoparticles. Adapted scheme from (Salata, 2004).

NPs are composed of three layers that are the surface, the shell and the core **(Figure 11)** (García-Pinel *et al.*, 2019). These layers confer less cytotoxicity, bio- and cytocompatibility, better conjugation with other bioactive molecules, and increase the dispersibility, thermal and chemical stability of NPs (García-Pinel *et al.*, 2019). The surface layer of NPs can protect and interact with other substances such as metals, polymers, surfactants or small molecules. The shell is an intermediate layer that can be porous or non-porous with specific chemical properties depending on your composition that are different from the core. The last layer of NPs, the core, is a portion that defines central position of NPs and can suffer chemical or thermal changes during exposure to surrounding environment **(Figure 11)** (Gawande *et al.*, 2015; García-Pinel *et al.*, 2019).

NPs can derive from natural or synthetic sources and can be classified into different groups according to morphology or shapes, characteristic colours, particle sizes, chemical properties and overall shapes (Khan, Saeed and Khan, 2017; Król *et al.*, 2017). Morphologies or shapes can provide a large surface area needed for good performance of NPs as catalysts and include quantum dots, nanotubes, nanospheres, nanowires, nanorods

nanobelts, and others **(Supplementary table 2)** (Murphy and Jana, 2002; F. A. Khan, D. Almohazey, M. Alomari, 2018). NPs can also adopt characteristic colours such white, wine red, yellowish-grey, black and dark black, different from the bulk materials, due to response to light transmitted or reflected light by the object. These colors are produced according to their modifications and the measure generally is made by surface plasmon resonance and quantum confinement depending of NPs composition material (Chhatre *et al.*, 2012; Ghasemi *et al.*, 2018). Accurately measuring the size of NPs in the defined particle size range is also made by different methods in order to ensure selectivity, sensitivity, limit of detection, limit of quantification, precision and trueness for material construction (K. G. Roebben J. Herrmann *et al.*, 2016) . Particle sizes can vary between 1mm to 100 mm. NPs size can affect drug release or polymer degradation. Smaller particles lead to the fast drug release (Pal *et al.*, 2011). Despite this, they tend to aggregate during storage and transportation of NPs dispersion. In bigger NPs the drugs diffuse more slowly (Pal *et al.*, 2011). The balance between particle size, drug release, drug loading, and maximum stability of NPs is, therefore, important for good characterization (Díaz and Vivas-Mejia, 2013; Kumar *et al.*, 2017). Chemical properties such as electronic, optical, magnetic, and mechanical, define the synergy promoting the efficient operation of NPs with unique characteristics for various applications. Optical characteristic is provided to give important information's about absorption, reflectance, luminescence and phosphorescence with fast, non-destructive and high resolution, which makes this an attractive property for materials´ characterization (Ghasemi *et al.*, 2018). The NPs ability to conduct flow through them is referred as electric property (Khan, Saeed and Khan, 2017). It can depend on the presence of electrons in solid materials and resistivity (Khan, Saeed and Khan, 2017). Magnetism is another parameter that characterizes NPs dependent on uneven electronic distribution (Pezeshki-Nejad *et al.*, 2019). Due to the small size and large surface to volume ratio of NPs, magnetism stay is dependent on surfaces and interphases that change the coordination number as well as change in the lattice constant giving rise to observation of ferromagnetic behaviour of materials. (Pezeshki-Nejad *et al.*, 2019). Finally, the mechanical comportment is a result of composition on bonds between the atoms, that can be covalent, metallic,

ionic; originating weak, strong or brittle pure materials and it can influence plasticity and hardness (D. Guo et al, 2014).

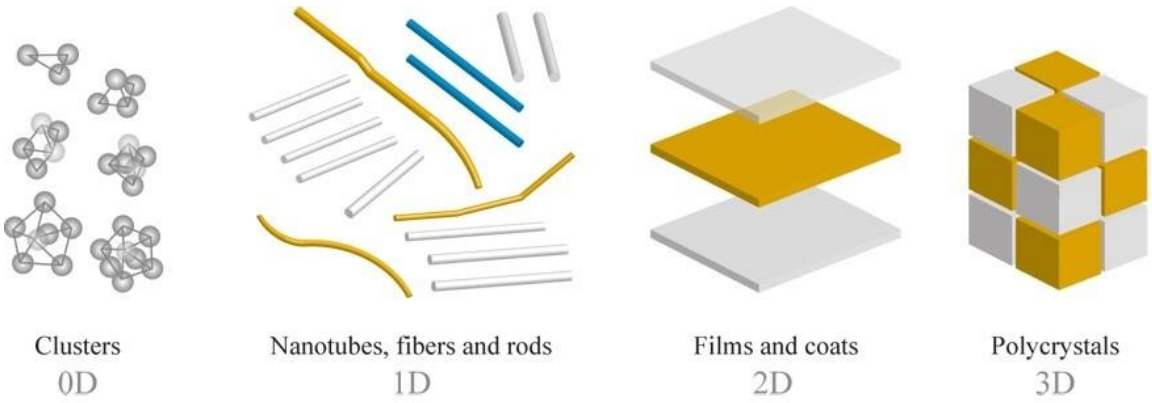

Figure 12 - Overall shape dimensions of nanoparticles and respective applications. NPs can be classified on zero (0D), one (1D), two (2D) and three (3D) dimensions according to overall shape.

NPs are classified based on zero (0D), one (1D), two (2D) and three (3D) dimensions according to overall shape **(Figure 12)** (Chen, Su and Jiang, 2019). For example, 1D NPs such nanowires or nanotubes have applications in biomedicine. (Pal *et al.*, 2011; Tiwari and Kim, 2012; Korayem *et al.*, 2017).

The final composition of NPs can involve organic or inorganic groups according to the description above and depending on the property analysed. It can constitute a novel drug delivery system to use in the different routes of administration, with the capability to deliver both hydrophilic and hydrophobic drug molecules.

2.2.2. Groups of nanoparticles

According to the type of material used in NPs synthesis, the most well-known NPs groups are designed by carbon, metal, ceramic, semiconductor, polymeric, and lipid-based NPs (LB NPs) **(Figure 13)** (Khan, Saeed and Khan, 2017).

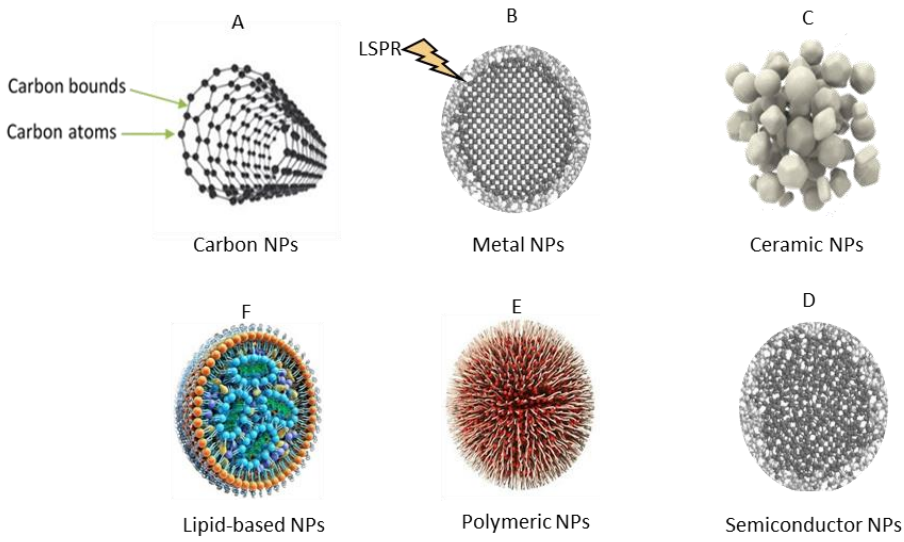

Figure 13 - Nanoparticles groups with different materials composition and respective structures. Depending of the type of material used in NPs synthesis, the most well-known NPs groups are designed by carbon **(A)**, metal **(B)**, ceramic **(C)**, semiconductor **(D)**, polymeric **(E),** and lipid-based NPs **(F)**. Adapted from (Adaptable Nanoparticle Research and Development, 2019)

Carbon NPs include, graphene, graphene oxide, fluorescent carbon quantum dots, diamonds, fullerenes, carbon nanotubes and graphite. They are composed by carbon atoms bounds which confer to carbon NPs high stability, good electrical and heat conductivity, low toxicity, environmental friendliness, high surface area and linear geometry (Yan *et al.*, 2016). Metal NPs, composed by pure metals like Au, Ag, Cu, Fe, Zn, have properties such mechanical strengths, high surface area, low melting point, magnetic properties and optical and electronic properties that arises from resonant oscillation of their free electrons in the presence of light. They are specific and dependent of the changes in the particle size, surface area of reactant and aggregation state. This increases reactivity to the reagent that makes up the dispersed agglomerates than the aggregate agglomerates, acting as a catalyst for chemical reactions. (Harish *et al.*, 2018). Ceramic NPs include particles made from oxides, carbides, phosphates, and carbonates of metals and metalloids such as calcium, silica, alumina, titanium, zirconia, silicon nitride, and silicon. These NPs are a group with magnetism, specific optical and dielectric properties, high heat resistance and chemical inertness whereby our synthesis occurs with heat followed by cooling (Thomas *et al.*, 2015). A semiconductor is a group of NPs derived from a variety of different compounds, referred to as II-VI, III-V, or IV-VI semiconductor nanocrystals, based on the periodic table into which these elements are formed (Kumar Sahu, 2019). They have interesting properties such narrow and intensive emission spectra, continuous absorption bands, high chemical and

photobleaching stability, processability, and surface functionality. (Kumar Sahu, 2019). Polymeric based NPs are formed from polymers with compositions, structures, and properties that allow developing efficient, tissue specific and nontoxic NPS. They make up different structures from capsules (polymeric NPs or polymeric nanoconjugates) to micelles (amphiphilic core/shell polymeric) and dendrimers (Moreno-Vega *et al.*, 2012). Lastly, -LBNPs such as liposomes, nanostructured lipid carriers and solid lipid NPs, belong to another group of NPs and they have characteristics are formed by the high loading capacity of hydrophobic and hydrophilic molecules, high temporal and thermal stability, very low or no toxicity, drug release control, increased of drug action time, ease of preparation, low production costs, and large-scale industrial production (Buse and El-Aneed, 2010; García-Pinel *et al.*, 2019).

2.2.3. Synthesis of nanoparticles

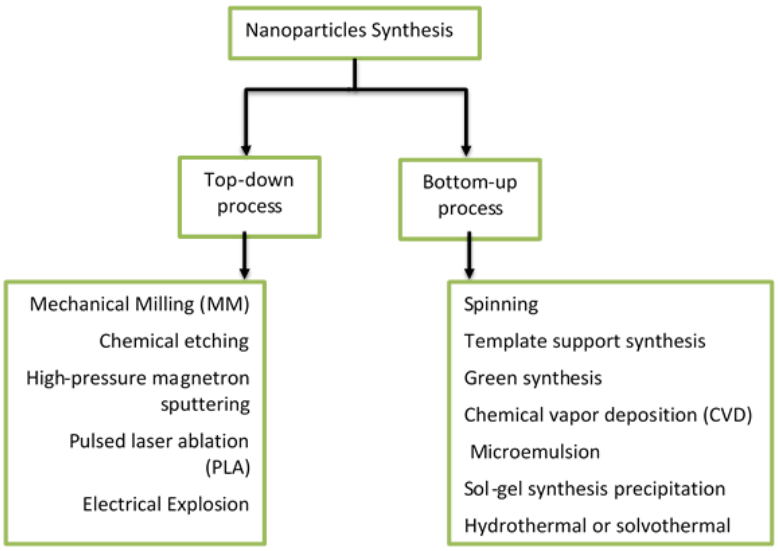

***Figure 14* - Summary of possible methods for ZnO NPs synthesis.** Synthetized of NPs occurs by two processes, top-down and bottom-up. The top-down process converts larger molecules into smaller ones. The bottom-up process converts simple substances in the complexed molecules. Adapted from (Wang and Xia, 2004).

All properties and specifications of NPs composition are employed by a set of physical, chemical and biological methods involved in NPs synthesis. These methods can develop NPs through two processes, top-down and bottom-up synthesis, which transform larger molecules in smaller units that are then converted into suitable NPS and simple substances in complexed molecules, respectively **(Figure 14)** (Wang and Xia, 2004). Beyond the

selection of the appropriated method, it is important to reflect on other important aspects, such as the selection of best organisms of NPs production according to intrinsic properties, appropriate conditions for cell growth, enzyme activity and optimal reaction conditions (Iravani, 2011). After stablishing these parameters, specific methods can act to modulate correctly the synthesis of NPs. Some methods of top-down process englobe mechanical milling, chemical etching, high-pressure magnetron sputtering, pulsed laser ablation and the electric explosion (Iravani, 2011; Khan, Saeed and Khan, 2017).

2.2.4. Zinc oxide nanoparticles

The diversity of properties between nanomaterials currently produced for numerous applications makes the difficult proper selection. In medical research, it is important to use NPs with adequate properties and whose sizes vary between 5-16 nm (Bogutska, Sklyarov and Prylutskyy, 2013). Therefore, nanometals such as magnesium, copper and Zn reveal a high-disperse powder. Complexating with organic compounds such as oxides appears to be benefical for biological activity (Bogutska et al., 2013; Khan et al., 2017a). Since Zn^{2+} is an active element and simultaneously a strong reducing agent, it can easily oxidize forming zinc oxide (ZnO). ZnO NPs are used given their biocompatibility, less toxicity and lower cost (Mishra *et al.*, 2017). Also the non-interaction of Zn^{2+} with the majority of pharmaceutically active molecules available, when compared with other metal oxide NPs makes them the most appropriate material for medical application (Mishra *et al.*, 2017). The production of ZnO NPs composite scaffolds suitable serves as a nerve guidance channel material by decreasing of astroglial cell density respectively (Hanley *et al.*, 2008; Webster, 2008). Nowadays, ZnO NPs are generally recognized as safe by US Food and Drug Administration (FDA) (Hanley *et al.*, 2008). It is a substance with specific properties of optical and chemical sensing, semiconducting, electric conductivity, piezoelectricity, transparency, high isoelectric point, biocompatibility, photocatalytic efficiency, high specific surface area, antibacterial and anticancer activities and ultraviolet -absorbing (Hanley *et al.*, 2008; Valdiglesias *et al.*, 2013).

ZnO NPs belong to metal and semiconductor groups, dimensions around 100 nm, a wide bandgap of 3.3 eV in the near-UV spectrum, high excitatory binding energy with 60 mV at

room temperature and their structures exist in two main forms, hexagonal and wurtzite (Król *et al.*, 2017). Different shapes of ZnO NPs including nanocombs, nanorings, nanohelixes, nanobelts, nanowires, and nanocages are available (Król *et al.*, 2017). They are synthesized by physical methods such laser ablation, thermal evaporation chemical methods such microemulsion, sol-gel synthesis, precipitation, thermal evaporation techniques such hydrothermal or solvothermal (Król *et al.*, 2017). Electrochemically, ZnO NPs can exhibit a type of surface charge behaviour that may vary due to their hydroxyl groups chemisorbed on their surface. Thus, at high medium pH, protons (H^+) move out from the particle surface in aqueous medium, leaving a negatively charged surface with partially bonded oxygen atoms (ZnO^-) (Król *et al.*, 2017). At lower pH, protons from the environment move into the particle surface resulting in a positively charged surface with partially bonded hid oxygen atoms ($ZnOH_2^+$) (Król *et al.*, 2017). Morphological forms and properties of nanostructured ZnO are employed in a variety of applications that include biology, medicine such bioimaging, drug and gene delivery and cosmetic industry such UV filters in sunscreens, toothpastes and mineral cosmetics. These NPs also be applied in manufacturing of materials such antimicrobial food packaging and protection from exposure to UV rays through industrial coats and antimicrobial textiles. They also have applications in energy and electronics such chemical sensors based on zinc oxide, low cost solar cells and nanogenerator power sensors based on ZnO nanowires (Valdiglesias *et al.*, 2013; Król *et al.*, 2017).

2.2.5. Zinc oxide nanoparticles on human health

ZnO NPs emerged to have a promising potential in several biomedical fields, namely; anti-cancer, anti-bacterial, anti-fungal, anti-diabetic and anti-inflammatory drug delivery systems as well as for application in bioimaging (Bisht and Rayamajhi, 2016).

At physiological conditions, ZnO NPs have an isoelectric point of 9/10, that allows a strong positive surface charge (Rasmussen *et al.*, 2010; Bisht and Rayamajhi, 2016). This creates an electrostatic interaction with a negative membrane potential of cancer cells promoting anticancer activity by cellular uptake, phagocytosis, and cytotoxicity of these NPs (Rasmussen *et al.*, 2010; Bisht and Rayamajhi, 2016). ZnO NPs can induce inhibition activity in a concentration-dependent manner in different ways between cell lines through loss of

cell viability and characteristic apoptotic features such as early and late apoptosis (Jiang, Pi and Cai, 2018; Arasu *et al.*, 2019). Anticancer effect of ZnO NPs has also been tested on different human cancer cell lines like colon, breast, lung, ovarian, cervical, gastric, human epidermal cancers to hepatocarcinome and acute promyelocytic leukemia (Jiang, Pi and Cai, 2018). In the outer membrane or cytoplasm of bacterial cells, there may also be accumulation of ZnO NPs and release of Zn^{2+}, leading to antibacterial activity (Jiang *et al.*, 2016; Jiang, Pi and Cai, 2018; S. Siddiqi, ur Rahman and Husen, 2018). In this interaction bacterial cells absorb Zn^{2+}, which inhibits the action of respiratory enzymes that generate ROS such superoxide anion, hydroxyl radicals and hydrogen peroxide (Jiang *et al.*, 2016; Jiang, Pi and Cai, 2018). ROS produces free radicals and consequently causes oxidative stress (Jiang *et al.*, 2016; Jiang, Pi and Cai, 2018). These NPs can create irreversibly conditions that promote bacterial cell membrane disintegration, membrane protein damage and genomic instability leading to the death of bacterial cells. (S. Siddiqi, ur Rahman and Husen, 2018) Other studies related to the antifungal activity of ZnO NPs in different fungal strains demonstrated that ZnO NPs can be toxic against some plant, food and human pathogens such as *Candida albicans*, *Aspergillus flavus* or *Aspergillus fumigatus* (N. O. Jasim, 2015; Hui, Liu and Ma, 2016; Barad *et al.*, 2017). ZnO NPs disrupt cell structure, block biological macromolecular activity and inhibit their synthesis, preventing DNA replication and disruption of the anti-oxidative system via ROS mediated Zn, which can be an advantage in combating infection, disease, biocontamination, and corrosion (N. O. Jasim, 2015; Hui, Liu and Ma, 2016; Barad *et al.*, 2017). ZnO NPs antimicrobial performance can be influenced by internal factors (e.g. particle size, concentration, morphology, structure and surface activity) or by external factors (e.g. photocatalytic efficiencies), thus affecting the viability of microorganisms in a concentration-dependent manner (Sun, Li and Le, 2018). Their role as an antidiabetic treatment was also investigated because of the ability of Zn^{2+} to maintain the structural integrity of insulin through its synthesis, storage, and secretion (Umrani and Paknikar, 2014). Adequate amounts of ZnO NPs were demonstrated to reduce blood glucose and increase insulin levels as well as improving serum zinc status in a time and dose-dependent manner (Umrani and Paknikar, 2014; Nazarizadeh and Asri-Rezaie, 2016). However, its administration triggered a severe increase in oxidative stress, particularly at the higher doses evidenced by the altered activities of the erythrocyte antioxidant enzyme, increased malondialdehyde production

and a marked reduction in serum total antioxidant capacity (Umrani and Paknikar, 2014; Nazarizadeh and Asri-Rezaie, 2016; Jiang, Pi and Cai, 2018). Hence, the efficiency must be improved by the combination of ZnO NPs with the antidiabetic drugs (Umrani and Paknikar, 2014; Nazarizadeh and Asri-Rezaie, 2016; Jiang, Pi and Cai, 2018). The anti-inflammatory properties of ZnO NPs have been widely reported (Mishra *et al.*, 2017). Penetration of ZnO NPs through the damaged epidermis into the viable layers of the injured skin allowed a reduction of skin thickness in the allergic environment, a suppression of inflammatory cells infiltration such T-cells, a downregulation of mRNA expression of different types of cytokines and an increase of IgE antibody levels (Ilves *et al.*, 2014). Drastically decreasing local skin inflammation and anti-inflammatory responses (Ilves *et al.*, 2014).

Finally, ZnO NPs show excellent luminescent properties turning them into one of the main candidates for bioimaging of human skin *in vitro* and *in vivo* (Mishra *et al.*, 2017). Due to their efficient blue emissions and near-UV emissions under the incidence of radiation, ZnO NPs provide comprehensive information in tumour diagnosis; thereby ZnO-based agents are very attractive for monitorization of therapy (Zhang *et al.*, 2013).

Research on ZnO NPs exposure in the central nervous system is scarce and studies are only targeted to toxicological, inflammation and oxidative stress impact on cells (Tian *et al.*, 2015;, 2018). In fact, ZnO NPs may improve the high toxic effects on neuronal cells due to their ion-releasing ability (Bisht and Rayamajhi, 2016; Yin, 2017). On the other hand, this severity of cytotoxicity can be controlled depending on the physicochemical properties acquired by ZnO NPs in their synthesis, such as chemical composition and small size (Shim *et al.*, 2014). These properties allow us to acquire optimal shape, state of aggregation and chemistry, energy and large surface area and penetrate the blood-brain barrier (BBB) (Shim *et al.*, 2014). The impact of ZnO NP-induced toxic response on oxidative stress and interactions of Zn^{2+} with their cellular targets is the major factor. Zn^{2+} shedding process can occur in the intracellular region. ((Liu *et al.*, 2017; Yin, 2017).

The use of ZnO NPs It can therefore be favourable for more accurate measurement of Zn^{2+} concentration within cells.

In this setting of the various effects conferred by ZnO NPs is important to investigate the consequence of exposing a neuronal model system to the former and start to unravel the

relevant underlying processes likely to be the molecular targets. This was the main goal of this thesis and the specific aims are described below.

3. Aims

Although zinc lacks redox activity and is regarded as relatively non-toxic, there is an increasing amount of evidence that free zinc ions may cause degradation of neurons. In this sense, Zn appears to be responsible for a variety of cellular responses from toxic to beneficial. Additionally, the form in which Zn is presented to cells may have a determining impact.

The main objectives of this thesis are the following:

- Optimize ZnO NPs exposure conditions to sub-toxicity effects using the SH-SY5Y neuronal cell line; in terms of both Zn concentrations and exposure times;
- Compare ZnO NPs and Zn^{2+} effect on SH-SY5Y cells to confirm their protective role in the CNS;
- Identify the molecular players involved in Zn^{2+} mediate responses at the synapse with special focus on the post-synaptic density at PSD-95, SHANK 3 and β-actin proteins levels.

4. Materials and Methods

4.1. Materials

4.1.1. Zinc oxide nanoparticles

NPs are an excellent material to apply to mammalian brain studies due to their properties and good capacity to pass through BBB (Martínez-Carmona, Gun'Ko and Vallet-Regí, 2018). ZnO NPs (Aldrich) were kindly provided by Prof. Ana Senos from Materials Department of University of Aveiro.

4.1.2. SH-SY5Y neuroblastoma cell lines

Preliminary research relevant to the mammalian brain can make use of *in vitro* cultures of neuronal cells. Once mammalian mature neurons do not undergo routine cell division, other secondary cell lines derived from neuronal tumours that have become immortalized are sought. These cellular models can grow easily in cell culture, ensuring unlimited cell numbers and minimizing variability between cultures (J. Gordon, S. Amini, 2014). Although they show many important physiological differences comparatively with the type of cell from which they were derived and care must always be taken when comparing to the human brain of the CNS as a whole (J. Gordon, S. Amini, 2014).

There are several established and well-characterized mammalian brain tumour cell lines available for the type of studies here presented. However, SH-SY5Y were chosen for this work because they have been extensively used in neuronal research and are very well characterized. Human SH-SY5Y cell line is a transformed neuron-like cell line type, subcloning from the parental metastatic bone tumour biopsy cell line SK-N-SH to SH-SY5 and finally to SH-SY5Y, by *J. Biedler* in the 1970's. It was obtained from ATCC with code ATCC CRL-2266 (Kovalevich and Langford, 2013).

4.1.3. Antibodies

Higher living organisms produce specific proteins by the immune system, called antibodies, through the biochemically process of degradation. They can protect host cells against

foreign invaders, called antigens. This biochemical process is a result of antibody-antigen association. This may occur through binding of Fab portion of the antibody with the epitopes of the antigen, creating chemical bonds that can be measured. In science, specific antibodies can be collected from the blood of many different animals. Then, they weresubject to immune system stimulation with antigens of interest. Antibodies are classified as monoclonal or polyclonal according to the epitope recognition capacity. Monoclonal antibodies contain a single antibody that are cloned from B-Cells. Therefore, they can recognize a single epitope from the antigen, which develop higher specificity despite less sensitivity. Polyclonal antibodies are instead a product of many different B-Cells binding in slightly different ways to the same antigen. These make them very impure products with a wide variety of antibodies.

In the present investigation, monoclonal antibodies were used for Western blot analysis. They were produced in mouse, according to conditions summarized in **Table 2** acquired from commercial sources as identified in the table.

Table 2 – Primary and Secondary antibodies used in this investigation and corresponding specifications.

Antibody Source	Molecular weight	Host	Type	Target	Dilution
Anti-PSD-95 (Alphagene)	95 kDa	Mouse	Monoclonal	PSD-95	1:2000
Anti-SHANK3 (Alphagene)	190 kDa	Mouse	Monoclonal	Shank 3	1:1000
Anti-β-Actin (Novus Biologicals)	45 kDa	Mouse	Polyclonal	β-Actin	1:5000
Anti-HRP (Cell Signaling)	-	Mouse	Polyclonal	Anti-mouse primary antibodies	1:5000

4.2. Methods

4.2.1. Synthesis and characterization of zinc oxide nanoparticles

ZnO NPs characterization was performed by Prof. Ana Senos ´s team. Briefly, ZnO NPs were prepared by dilute zinc acetate in ethanol followed by evaporation in a rotary evaporator. The average particle size determined by transmission electronic microscopy was less than 35 nm and appeared as aggregated hexagonal shaped particles. Briefly, ZnO NPs were diluted in the initial concentration of 2000 mg/mL in phosphate buffered saline (PBS) and mantained at 4 ^{o}C. Before each application, they were tip sonicated for 5 minutes. They underwent different dilutions (0.0, 0.1, 0.5, 1.0, 10.0, 50.0 and 100.0 mg/mL) were dissolved in complete medium and mixed to ensure correct dilution. Sterilization with U.V. radiation was carried out before each dilution.

4.2.2. Human neuroblastoma cell line (SH-SY5Y) cells culture

Human SH-SY5Y cells (ATCC CRL-2266) were plated, grown and maintained in minimal essential medium (MEM)/F12 (1:1) supplemented with 10 % fetal bovine serum (FBS), 0.5 mM L-glutamine, 45 mM sodium pyruvate, 100 µg / mL penicillin and 100 mg / mL streptomycin (Kovalevich and Langford, 2013). Cultures were maintained in a humidified chamber at 37˚C under 5 % CO_2. Cells were sub-cultured when 80-90% confluence was reached and plated into 6-wells or 96-wells plates according to the different experimental conditions as explained below.

4.2.3. Viability assay

SH-SY5Y cells were seeded at a density of 2.0×10^4 cells/well in a 96-well plate; counting was performed by staining with the trypan blue dye. Cells were cultured in complete medium during 24 hr. Then, cells were exposed to different concentrations of ZnO NPs (0.1, 0.5, 1.0, 10.0, 50.0, 100.0 µg/mL) in a final volume of 100 µL/well at different timepoints (2, 4, 6, 12, 24 hr). Resazurin was added to cells for 2 or 3 hr at final concentration of 10

µg/mL. The cellular uptake was analysed using a microplate reader 570/600 nm as the excitation source, to monitor the absorbance intensity.

4.2.4. ROS assay

Living cells are continuously exposed to oxygen and produce reactive oxygen species (ROS) through respiratory metabolism, especially from mitochondria. ROS are reactive chemical species present in cellular signalling machinery. They have action in several biological processes such as cellular proliferation, differentiation, migration and homeostasis maintaining. ROS levels are regulated by antioxidants such glutathione (GSH) (Hancock', Desikan and Neil, 2001). They have different properties which allow to distinguish them in two species, less reactive oxygen species (loROS) and highly reactive oxygen species (hiROS) (Hancock', Desikan and Neil, 2001). LoROS such as superoxide and particularly hydrogen peroxide, participate in cellular signalling. hiROS, such as the hydroxyl radical or peroxynitrite, can damage all types of biological molecules and change mitochondrial functions (Hancock', Desikan and Neil, 2001). This results in oxidative damage to lipids, proteins and DNA, as is commonly observed in neurodegenerative disorders. In the nervous system, studies of ROS revealed that synaptic and non-synaptic mitochondria have different protein compositions, respiration rates and generate different amounts of ROS. All this can influence neuronal development and function through establishment of neuronal polarity, regulation of cytoskeletal changes and modulation of neuronal growth and plasticity. In neurodegenerative diseases, metabolic conditions are altered by increasing ROS or oxidative stress induction (Hancock', Desikan and Neil, 2001). These alterations result in cellular damage and deficiencies in the development and function of neuronal transmission (Hancock', Desikan and Neil, 2001). According to the literature induction of ZnO NPS in neuronal cells has been proved to increase ROS levels generated. Therefore, it is reasonable to test the relative amount of ROS produced by cells in culture. For this, SH-SY5Y cells were plated at cellular density of 2,0 x 10^4 for 24hr of incubation. Cells were treated with 100 µL/well of different concentrations of ZnO NPs (0,1; 0,5; 1; 10; 50; 100 µg/mL) in 96-well plate for different timepoints of incubation (2, 4, 6, 12, 24 h) at 37°C. Then, ROS was measuring using the ROS/Superoxide Detection Assay Kit (ab139476) from Abcam that detects comparative levels of total ROS (Microscopy and Cytometry,

2016). The ROS Assay kit was included a probe with an oxidative stress detection reagent. This reagent was reconstituted in 60 µL of DMF anhydrous for an initial stock solution of 5 mM. After that, it was diluted in completed medium for a final dilution of 1:250. It was applied to the cells at the final concentration of 1: 2500 in order to react with a wide range of reactive species. The reaction generated a green fluorescent product that was visualized in a wide-field fluorescence microscope equipped with standard green **(Ex/Em = 490/525 nm)**. As a positive control 100 µL of Pyocyanin was added in each well that was reconstituted in 100 µL of DMF anhydrous as a stock solution of 10mM. Therefore, it was diluted in completed medium for a final concentration of 200-500 µM. A negative control, N-acetyl-L-cysteine, was also applied to cells in 100 µL after being reconstituted in 123 µL of de-ionizated water for a stock solution 0,5 M. Finally, it was diluted in medium to a final concentration of 5 mM.

4.2.5. Lysate collection

To extract proteins from mammalian SH-SY5Y cells, it was necessary to carry out cell lysis, that were previous plated and treated as described in 4.2.3.. Radioimmunoprecipitation assay (RIPA) buffer to enable the extraction of membrane nuclear and cytoplasmic proteins was used, since it contains sodium dodecyl sulfate (SDS), a strong ionic detergent capable of promoting membrane disruption. SDS leads to full cell lysis and solubilizes lipids and proteins, thus it was mixed with 100 µM Na_3VO_4 (sodium orthovanadate), 1 M of NaF (sodium fluoride**)** and a protease inhibitor cocktail (complete, EDTA-free, Roche, cat #11873580001) to prevent proteolysis, dephosphorylation and denaturation of proteins.

After the appropriate treatments, cells at a density of 9.0 x 10^4 were washed in ice-cold PBS, and then collected from each well with RIPA lysis buffer. The cells of each well were collected with the help of a scrapper and resuspended with a micropipette. The contents were transferred to a microtube, sonicated twice for 5 seconds and maintained at -20°C.

4.2.6. BCA assay

The BCA protein assay is the most popular detergent-compatible formulation based on Pierce's bicinchoninic acid (BCA) for the colorimetric detection and quantitation of total protein. This method is based on the capacity of protein to reduce Cu^{2+} in Cu^{+} in an alkaline medium. The reaction is a biuret reaction because it presents highly sensitive and selective colorimetric detection of the cuprous cation (Cu^{+}) using a unique reagent containing BCA. Conversion is observed by modification of colour reagent from green to purple.

Table 3 - Protein standards performed in the BCA Assay.

P_0	BSA 2mg/mL (uL)	SDS 1% (uL)	Protein mass (ug)
P_0	0	25	0
P_1	1	24	2
P_2	2	23	4
P_3	5	20	10
P_4	10	15	20
P_5	20	5	40

In this assay, a Pierce^{TM}BCA protein assay kit (Thermo Fisher Scientific, cat. #23225) was used in which five standards samples according to **Table 3**, with known concentrations of bovine serum albumin (BSA) were prepared in a 96-well plate. Additionally, samples of the cells experimental lysates were also prepared by mixing 5 µL of each sample lysate with 20 µL of SDS 1 %. All samples were prepared in duplicate. At the end, 200 µL of working reagent (WR) was added to each well. The WR was prepared by mixing A and B reagents of the BCA kit in 50:1 proportion. The plate was incubated at 37°C for 30 minutes and absorbance was measured at 562 nm using a microplate reader (Infinite M200, TECAN). To determine protein concentration, a standard curve was calculated by plotting standard absorbance vs standard BSA concentration.

4.2.7. Western blot

Western blot technique, also called protein immunoblot, consists in detecting specific proteins in using specific antibodies. Cell lysates are collected after exposure to the different treatments and processed using adequate equipment (Biosciences, 1999; Bio-Rad, 2019). This technique includes three main steps, (1) gel electrophoresis, (2) blotting/transfer and (3) detection (Biosciences, 1999; Bio-Rad, 2019). The electrophoresis separates different proteins according to size through an sodium dodecyl sulphate polyacrylamide gel (SDS-PAGE) composed by two distinct layers of gels, a resolving gel **(Supplementary table 4)**, in the bottom, with a higher polyacrylamide concentration to separate proteins and a packaging gel, on the top, with a lower polyacrylamide concentration **(Supplementary table 5)**. The blotting or transfer proteins occurs onto a solid support, like a nitrocellulose membrane. Finally, the detection that immunolabels the target protein using a suitable primary and secondary antibody permits direct visualization of the proteins of interest (Biosciences, 1999; Bio-Rad, 2019).

4.2.7.1. Gel eletrophoresis

Protein samples were separated based on size using a Hoefer electrophoresis system and SDS-PAGE gels, enabling the subsequent estimation of the molecular weight of the proteins of interest. For this work, SDS-PAGE was prepared with a resolving gel composition of 7,5 % of acrylamide and packaging gel with 3,5 % of acrylamide **(Supplementary table 4, 5)**. At the same time, while gels polymerized, samples were prepared by adding 40 µL of protein solution, ¼ volume of Loading Buffer 4x (LB) to a final volume of 160 µL. LB is a component that increases sample density, masking any inherent protein charges, breaking disulphide bonds, thus disrupting quaternary and tertiary structures. It also allows sample tracking and progression in the gel **(Supplementary table 6).** Once prepared, mixed samples were boiled for 5 minutes and 150 µL, loaded onto the polymerized gels alongside a molecular weight marker, Precision Plus Protein Dual Color Standards, from BioRad. An electrical current with 90mA was applied for 3-4 hrs. After separation, the SDS gel with proteins was transferred to a nitrocellulose membrane using standard procedures for 18 hours **(Supplementary table 7)**. This process allows immobilization of all proteins onto nitrocellulose membranes at their relatively migration positions, from negative pole to

positive pole. Membranes were then hydrated for 5 minutes with Tris Buffered Saline (TBS) 1x **(Supplementary table 8).** Stained with a Ponceau S. for 5 minutes, which confirmed protein transfer. Membranes were washed with de-ionized H_2O to remove excess Ponceau solution and photographed using a colorimetric program of Chemidoc XR machine from BioRad. Finally, membranes were washed with Tris Buffered Saline Tween (TBS-T) 1x (0.5 % Tween). In all processes the membranes were constantly shaking to improve the effectiveness of the experiment.

4.2.7.2. Blotting

For immunodetection, membranes were washed with shaking twice for 5 minutes in TBS 1x and blocked with 1.5 % of BSA or 5 % of non-fat milk for SHANK 3 and PSD-95 respectively. This step blocked non-specific sites of the primary antibody. Upon 1.5-2 hr of incubation with a blocking solution, membranes were incubated with 20 mL of specific primary antibody overnight at 4˚C in the case of Anti-PSD-95 and Anti-β-actin antibodies. For anti-SHANK 3 antibody, incubation occurred for 2 hr at room temperature, with shaking. After that, membranes were washed with TBS-T 1x six times for 5-10 minutes each with shaking. Then, they were incubated with an Anti-HRP mouse secondary antibody reconstituted in 5 % of milk for 1hr at room temperature with shanking. Finally, membranes were washed with TBS-T 1x six times for 5-10 minutes with shanking.

4.2.7.3. Detection

After secondary antibody binding, the horseradish peroxidase in the proteins conjugated with the secondary antibody, catalysing the oxidation of luminol. The oxidation process emitted light detected by chemiluminescence. The detection occurred through the application of an enhanced luminescence (ECL) detection kit over the membrane for 1 minute. This signal was detected using the Chemidoc XR, BioRad resulting in images with specific bands. Bands were further analysed with Image Lab, BioRad to obtain a quantification of the intracellular protein levels.

4.2.8. Statistical Analysis

Statistical analysis was performed using GraphPad Software. Statistical significance was assessed using the one-way ANOVA analysis of homogeneity of variance, assuming Guassian distribution. The Bonferroni test was used for multiple comparisons of confidence intervals and significance, when equal variance was assumed and homogeneity was not verified, respectively. *P* value was considered significant when less than 0.05 to indicate statistical significance compared with the mean of the corresponding control group. Experimental data were expressed as means ± standard error of the mean (SEM) of at least three independent experiences.

5. Results

5.1. Effect of Zn^{2+}on SH-SY5Y cells viability

5.1.1. Influence of zinc oxide nanoparticles in SH-SY5Y cell viability

In order to test sub-toxic concentrations of ZnO NPs in SH-SY5Y cells, neuroblastoma cells were treated with different concentrations of ZnO NPs (0.0, 0.1, 0.5, 1.0, 10.0, 50.0 , 100.0 µg/mL) and for different times (2, 4, 6, 12 and 24 hr) **(Figure 15).** Cell viability was measured using the resazurin solution as explained in section 4.2.3.

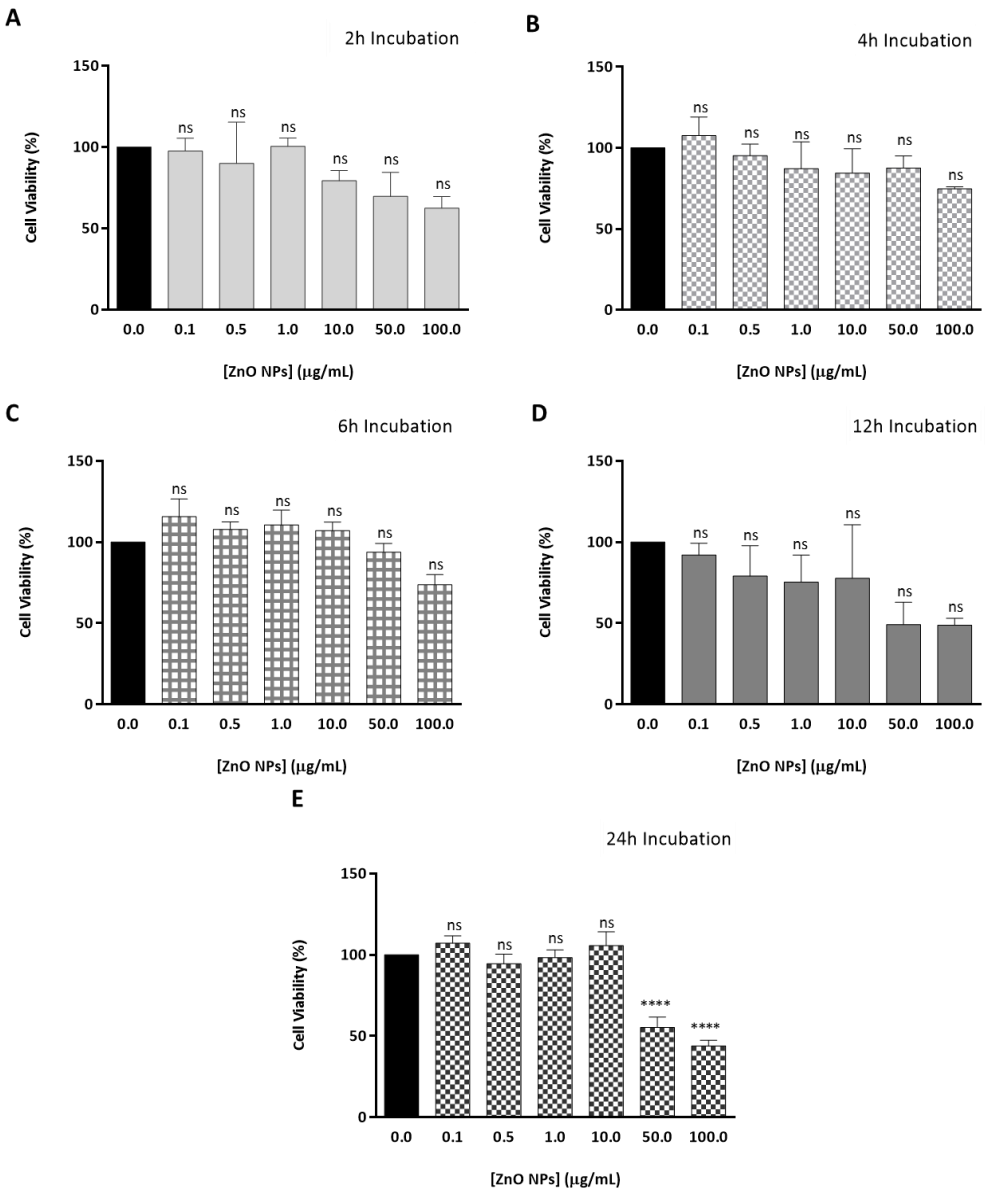

Figure 15 - Effects of ZnO NPs on SH-SY5Y cells' viability. (A-E) Percentage of SH-SY5Y viability was measured using the resazurin solution after cells were exposed to different ZnO NPs concentrations (0.0, 0.1, 0.5, 1.0, 50, 100 µg/mL) and different incubation periods, 2 **(A)**, 4 **(B)**, 6 **(C**), 12 **(D)** and 24 **(E)** hours respectively. Cell viability was expressed as a function of control, where control was a set as 100%. Graph bars correspond to the mean of viable cells, percentage against control, for each ZnO NPs concentration tested with the respective SEM. Results are represented as a viability percentage change over control. P values is <0.05, **** < 0,0001 **(E)**. ns, not-significant, N=3 (8 replicates per trial).

According to treatment conditions, an overall negligible decrease in cell viability was observed with increasing concentration and incubation time of ZnO NPs. **Figure 15 A** show an overall decrease in cell viability with concentration, when cells are incubated for 2 hours. After 4 hours of ZnO NPs exposure, no significant differences were detected in cell viability. However, there seems to be a tendency to decrease with the increased nanoparticles concentration **(Figure 15 B)**. Similar results were observed in cells treated with ZnO NPs during 6 hr. A sharp decrease, although not significant, was registered at 50.0 and 100.0 µg/mL **(Figure 15 C)**. When cells were exposed for 12 **(Figure 15 D)** and 24 hours **(Figure 15 E)** of incubation, the decrease in viability with concentration becomes clearer. This decrease is statistically significant at 24 hr of incubation and at concentrations of 50.0 and 100.0 µg/mL **(Figure 15 E)**.

To summarize, no significant variations in cell viability in the shorter times were noted. At periods longer than 12 hrs, however, the results demonstrated that higher concentration of ZnO NPs could influence the cellular homeostasis.

For subsequent experiments, 0.1 µg/mL and 0.5 µg/mL ZnO NPs concentrations were used as the most appropriate least toxic cell conditions due to their negligible variation in viability.

As a supplement, **Supplementary figure 1** summarizes all effects on cell viability observed with varying times and concentrations.

5.1.2. Influence of zinc oxide nanoparticles on SH-SY5Y cell ROS production

Another parameter important to measure, was to establish if Zn^{2+} also affects the mitochondrial system. In fact, ROS production may be an effective parameter to detect the impact of the proposed treatment due to the deleterious effects of aerobic respiration.

The production of ROS was thus evaluated according to the formulation and procedure described in section 4.2.4., using previously defined conditions set up in the laboratory **(Figure 16).**

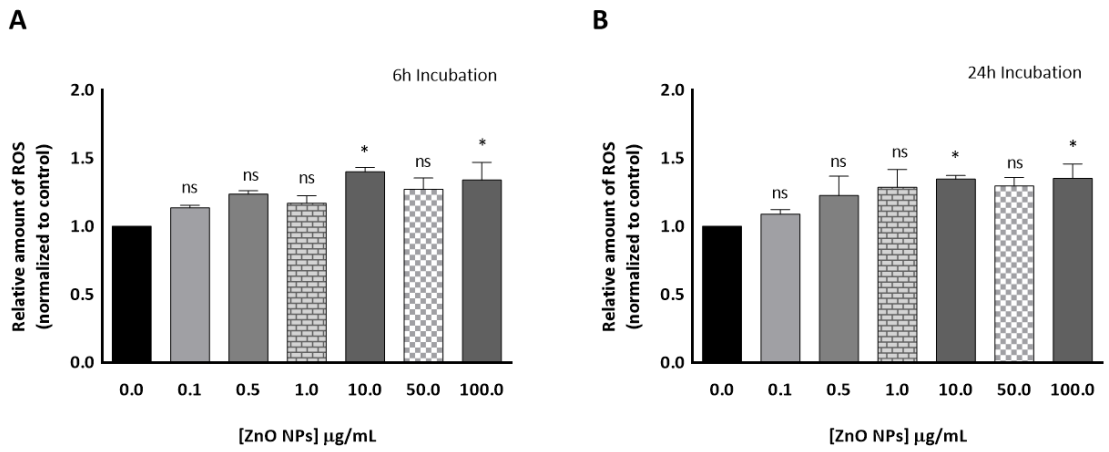

Figure 16 - Effects of ZnO NPs on SH-SY5Y cells' ROS production. Relative amount of SH-SY5Y ROS was measured using a ROS kit solution after cells exposure to different ZnO NPs concentrations (0.0, 0.1, 0.5, 1.0, 50, 100 µg/mL) during different incubation times, 6 **(A**), and 24 **(B)** hours respectively. Graph bars correspond to the mean of relative amount of ROS for each ZnO NPs concentration tested with the respective SEM. Results are represent as a ROS production over control. P values is <0.05, *= 0,0267 for 10.0 0 µg / mL; *= 0,0200 for 100.0 0 µg / mL **(A)**; * 0,0494 for 10.0 0 µg / mL; *= 0,0209 for 100.0 µg / mL **(B)**. ns, not-significant, N=2 (8 replicates per trial).

To summarize, it was evident that ZnO NPs produced an increase in ROS production when cells were exposed for 6 hours **(Figure 16 A)** and 24 hours **(Figure 16 B)**. The increase seen was significant when cells were exposed to treatment of 10.0 and 100.0 µg/mL ZnO NPs at both exposure times.

The increase was not significant for ZnO NPs concentrations, 0.1 and 0.5 µg / mL, previously selected in the viability assay, and as recorded in section 5.1.1. Thus, these results validate the possibility of using these concentrations for further assays.

5.1.3. Comparative effect between zinc oxide nanoparticles and zinc sulphate treatments in SH-SY5Y cells viability

To compare the effect of ZnO NPs and free Zn^{2+} ($ZnSO_4$) in SH-SY5Y cells, a resazurin assay also performed to evaluated cell viability after the different treatments **(Figure 17).**

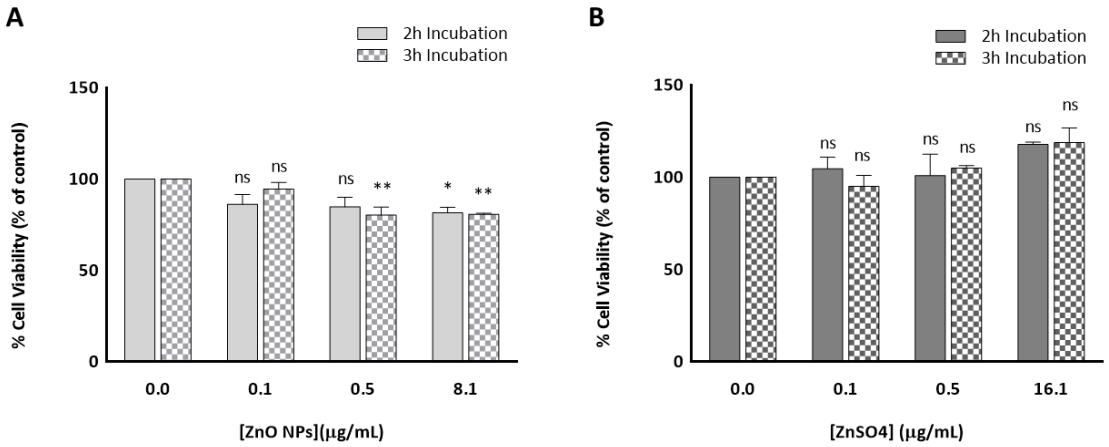

Figure 17 - Comparative effect of ZnO NPs and $ZnSO_4$ treatments on SH-SY5Y cells' viability. SH-SY5Y cells were treated with different concentrations of ZnO NPs or $ZnSO_4$ for 2 or 3 hours. Percentage of cell viability was measured using a resazurin solution, following cell treatments with 0.0, 0.1, 0.5 and 8.1 µg/mL **(A)** of ZnO NPs or 0.0, 0.1, 0.5 and 16.1. µg / mL **(B)** of $ZnSO_4$. Graph bars correspond to the mean of viable cells percentage for each ZnO NPs or $ZnSO_4$ concentration tested with the respective SEM. Results are represent as a percentage change over control. P values is <0,05, ns, not-significant, N=3 (8 replicates per trial).

Previous results from our laboratory showed that $ZnSO_4$ revealed a non-toxic effect at a concentration of 100.0 µM for 3 hours. Based on this, and in addition to the previous concentrations of 0.1 and 0.5 µg/mL defined above, another concentration was included to be tested with ZnO NPs and $ZnSO_4$ which, considering the molecular weight differences, corresponds to 8.1 µg/mL and 16.1 µg/mL, respectively.

The results showed a toxic effect of ZnO NPs treatment on SH-SY5Y cells with an increase in the concentration **(Figure 17 A).** This toxic effect was more significant at 0.5 µg/mL concentration after 3hr incubation and at 8 µg/mL concentration for both incubation times. However, between the two incubation times, in general, no relevant differences were observed. In $ZnSO_4$ treated cells, an insignificant increased was observed in SH-SY5Y cells viability with time and concentration **(Figure 17 B).** In conclusion, ZnO NPs exert a more toxic effect that $ZnSO_4$ at the concentrations tested.

5.2. Effect of zinc oxide nanoparticles on neuronal proteins levels

Zn^{2+} has an important function in several transduction signal pathways in post-synaptic terminals. So, in order to explore the role of ZnO NPs at this sub-cellular localization, SH-SY5Y cells were treated with ZnO NPs at the previously selected concentrations, 0.1 and 0.5

µg/mL, for incubation times of 10, 30, 60 and 120 minutes. SHANK 3, PSD-95 and β-actin levels were evaluated due to their important roles in modulating glutaminergic synapses.

Results showed variations in the levels of some of the tested proteins, once the blots were normalized against Ponceau S. staining **(Supplementary figure 2)**.

5.2.1. Changes in PSD-95 protein levels

For PSD-95, the expression levels were recorded over the increasing incubation time for the two concentrations tested **(Figure 18).**

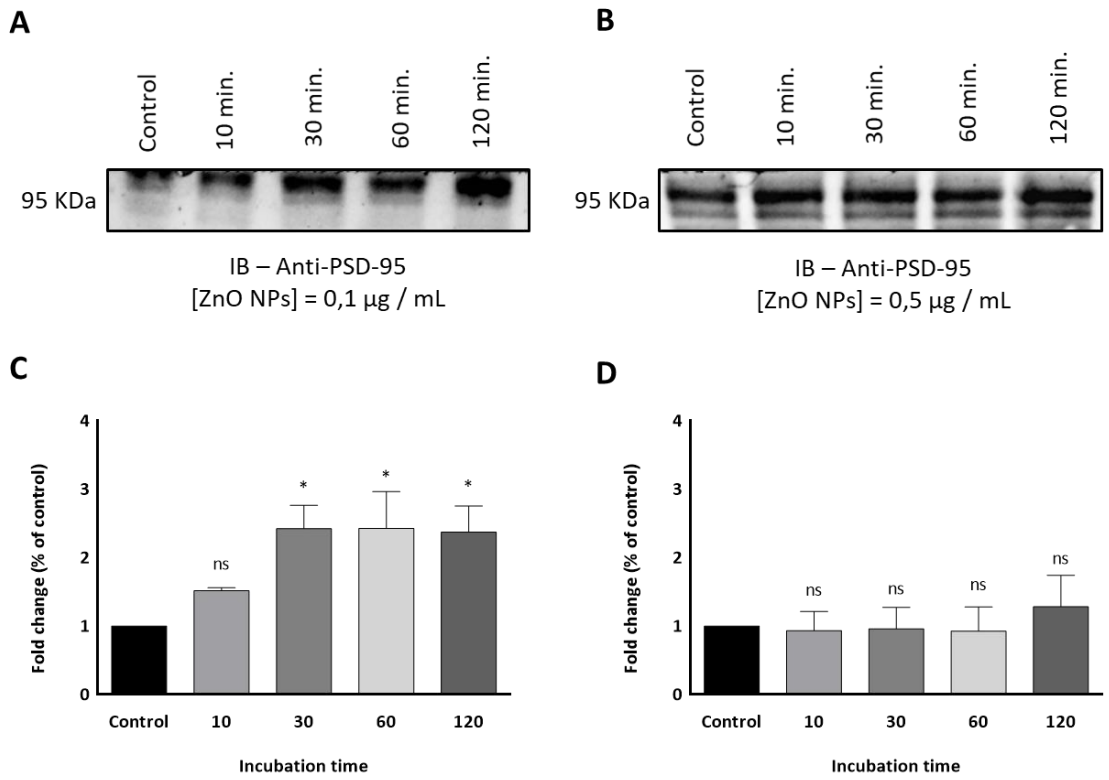

Figure 18- PSD-95 expression levels in SH-SY5Y cells treated with ZnO NPs at incubation times of 10, 30, 60 and 120 minutes. Western blot analysis of SH-SY5Y lysates exposed to treatment with 0.1 µg / mL **(A)** and 0.5 µg/mL **(B)** of ZnO NPs and quantification of PSD-95-fold changes **(C and D, respectively).** Graph bars correspond to the mean of PSD-95 protein levels for each concentration tested with the respective SEM. Blots were normalized to Ponceau S. and results are represent as a fold change over control. P values is < 0,05, * = 0,0189 for 30 minutes, * = 0,0185 for 60 minutes and * = 0,0242 for 120 minutes **(C)** ns = non-significate, N=5.

A not-significant increase in PSD-95 levels was observed for concentration of 0.1 µg/mL at shorter periods, but becoming significant after exposure times of 30, 60 and 120 minutes **(Figure 18 A, C).** Treatment with 0.5 µg/mL ZnO NPs revealed no significant variation in protein levels **(Figure 18 B, D)**. There was, however, a slight increase at 120 minutes of exposure treatment. **(Figure 18 B, D)** It can be concluded that treatment with ZnO NPs at

0.1 µg/mL appears to exert more changes in the PSD-95 expression when compared to treatment with 0.5 µg/mL. However, this needs to be further validated.

5.2.2. Changes in SHANK 3 protein levels

SHANK 3 levels were then analysed after exposure to the same set of conditions. A tendency to increase was observed with time **(Figure 19).**

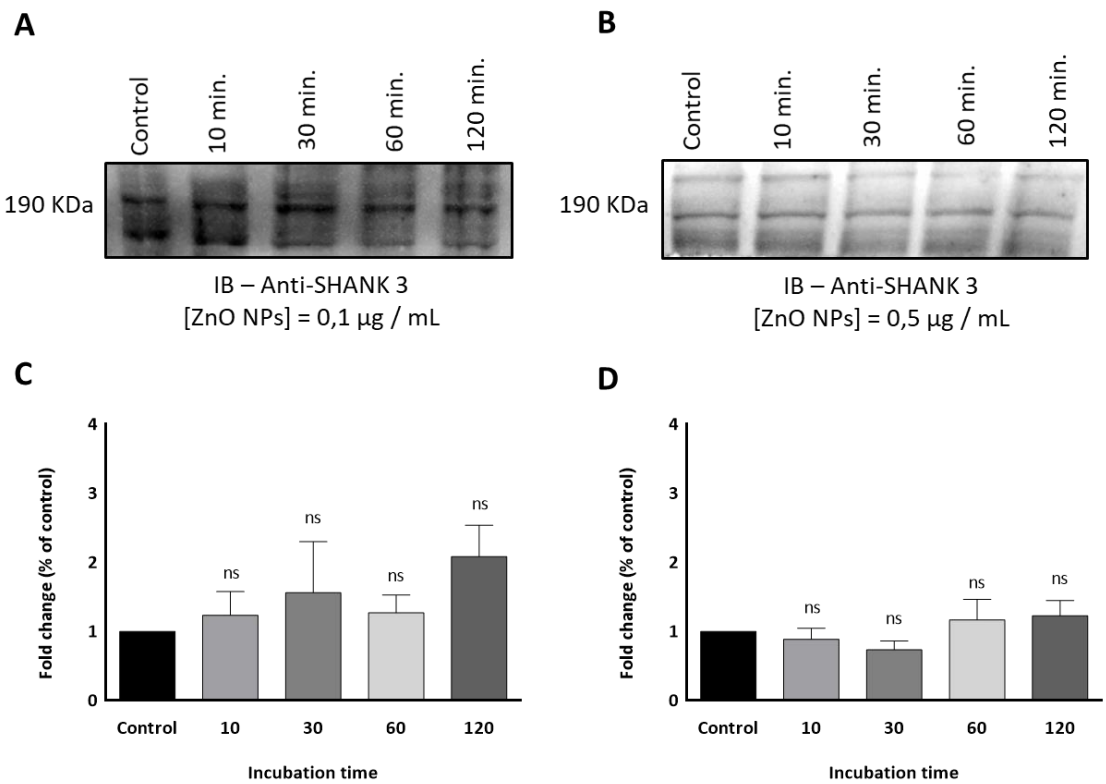

Figure 19 - SHANK 3 expression levels in SH-SY5Y cells treated with ZnO NPs at incubation times of 10, 30, 60 and 120 minutes. Western blot analysis of SH-SY5Y lysates exposed to treatment with 0.1 µg/mL **(A)** and 0.5 µg/mL (**B)** of ZnO NPs and quantification of SHANK 3-fold changes **(C and D respectively)**. Graph bars correspond to the mean of SHANK 3 protein levels for each concentration tested with the respective SEM. Blots were normalized to Ponceau S and results are represented as a fold change over control. P values is < 0,05, ns=not-significant, N=5.

Indeed, treatment of the neuroblastoma cell line with 0.1 µg/mL ZnO NPs appeared to induce a progressive increase in SHANK 3 protein expression with incubation time. A small decrease in protein expression was seen at 60 minutes, however, this was not significant **(Figure 19 A, C)**. At 0,5 µg/mL ZnO NPs concentration no significant differences were observed when compared with non-treated cells **(Figure 19 B, D).** Comparing the graphs of figures 20 C and 20 D for the two ZnO NPs treatments tested, it was also possible to see the influence of ZnO NPs concentration on the protein expression. At 0.1 µg/mL of ZnO NPs

concentration, an increased in protein levels was observed, while for 0.5 µg/mL there is a change towards a decrease.

5.2.3. Changes in β-actin protein levels

Finally, an immunoblot was performed to analyse the β-actin levels **(Figure 20).**

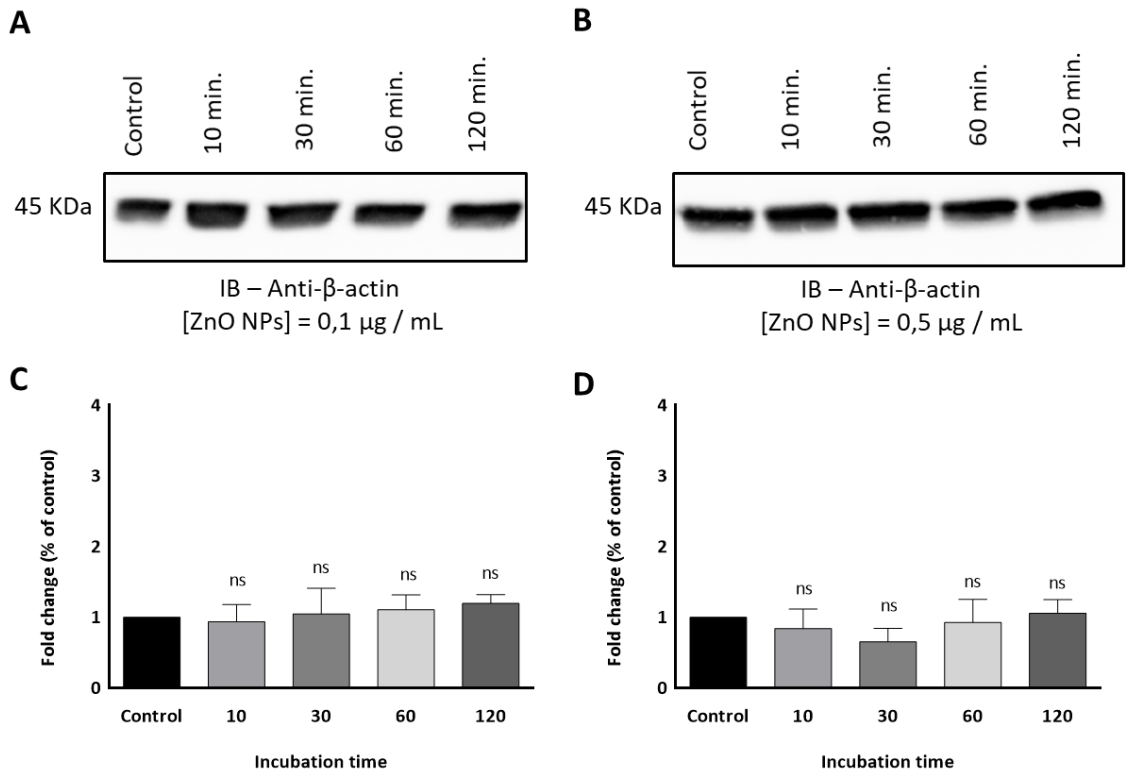

Figure 20 - β-actin expression levels in SH-SY5Y cells treated with ZnO NPs at incubation times of 10, 30, 60 and 120 minutes. Western blot analysis of SH-SY5Y lysates exposed to treatment with 0.1 µg/mL **(A)** and 0.5 µg/mL (**B)** of ZnO NPs and quantification of β-actin-fold changes **(C and D respectively).** Graph bars correspond to the mean of β-actin protein levels for each concentration tested with the respective SEM. Blots were normalized to Ponceau S and results are represented as a fold change over control. P values is < 0,05, ns=non-significate, N=5.

No significant variations in protein expression were observed when cells were exposed to ZnO NPs concentration of 0.1 µg/mL **(Figure 20 A, C).** A small decrease after 10 and 30 minutes was noted in cells treated with 0.5 µg/ml ZnO NPs, although this was not significant **(Figure 20 B, D).**

6. Discussion

The mode of action of Zn^{2+} as ZnO NPs was tested in SH-SY5Y cell-based neuronal system to evaluate, under sub-toxicity conditions, variations in key post-synaptic protein levels.

It was demonstrated that ZnO NPs can have possible beneficial effects on the increase of some important proteins in signaling pathways in the CNS. Sometimes these proteins are altered in neurodegenerative diseases. An interaction between Zn^{2+} and SAM domain of SHANK 3 protein with other components of PSD has been described (Arons *et al.*, 2016). Among several SHANK protein associations, binding to the NMDA receptor by the SHANK-GKAP-PSD-95 complex with consequent binding to neuroligin-neurexins influences neuronal synthesis and synaptic modulation (Meyer *et al.*, 2004; Romorini *et al.*, 2004; Futai *et al.*, 2007; Petralia, Al-Hallaq and Wenthold, 2008).

The studies here presented focussed on the influence of ZnO NPs on the levels of SHANK3, PSD-95 and β-actin expression. In signaling pathways, these three important proteins are involved in synaptic communication. The use of ZnO NPs is particularly relevant as the latter can pass BBB in the human brain and enable the interaction of Zn^{2+} with these PSD proteins. Besides appearing to cause variations in protein expression levels, it also influences the establishment of new functional excitatory synapses (Shim *et al.*, 2014).

Other previous studies identified sub-toxic concentrations of ZnO NPs in SH-SY5Y cells. It was demonstrated that for concentrations above 40 μg/mL a decrease in cell viability was observed (Liu *et al.*, 2017). Furthermore, no toxic effects after 2 hours of treatment exposure was observed but, when cells were treatment and exposed for 24 hours, cell viability showed a significant decrease (Liu *et al.*, 2017). In this thesis, in order to find the sub-toxicity concentrations of ZnO NPs treatment in SH-SY5Y cells, the viability assay was performed, with exposure periods of ZnO NPs for 2, 4, 6, 12 and 24 hours and at 0.0, 0.1, 0.5, 1.0, 10, 50.0 and 100.0 μg/mL concentrations. Results suggest that ZnO NPs has a minor toxic effect at concentrations below 50 μg/mL and at incubation periods of less than 6hr. This supports the data described in the literature (Liu *et al.*, 2017). Among the concentrations tested, 0.1 μg/mL was found to be the most suitable concentration to be used for further experiments as it has a low detrimental impact on cell viability. Another concentration, 0.5 μg/mL, was also used as a comparison due to the small difference between these two concentrations.

A viability assay was performed in all cases, to compare the efficiency of two treatments, ZnO NPs and $ZnSO_4$, on cell viability. The results revealed that the protective role of NPs was greater than that of free Zn^{2+}. A higher toxic effect of ZnO NPs compared to treatment with $ZnSO_4$ for time exposures tested was evident, and significant for ZnO concentrations above of 0,5 µg/mL and at 3 hr of incubation. According to the literature, Zn^{2+} in the synaptic cleft at concentrations above 100 µM is enough to effectively modulate synaptic function though pre- and post-synaptic pathways (Pivovarova *et al.*, 2014). On the other hand, extracellular Zn^{2+} concentrations between 30-1000 µM induce intracellular Zn^{2+} elevation and subsequent neuronal death during neuronal depolarization (Canzoniero, Turetsky and Choi, 1999). Studies conducted to assess the impact of Zn salts on neuronal cells also showed the effects of Zn^{2+} entry into cells. Results only have significance for Zn^{2+} salt concentrations greater than 100 µM and for periods greater than 2 hr (Pavlica, Gaunitz and Gebhardt, 2009; Pavlica and Gebhardt, 2010). In addition, because of their unique characteristics, ZnO NPs require some form of endocytosis to cross the cellular membrane and Zn^{2+} within the ZnO NPs are dissolved in culture medium or inside the cells due to the low pH of endosomes and phagosomes (Turney *et al.*, 2012). This process results in the elevation of free intracellular Zn^{2+} and in cytotoxicity for neuronal cells. The same does not occur for $ZnSO_4$ because its free Zn^{2+} remains outside the cells, forming poorly soluble amorphous Zn-carbonate phosphate precipitates that protect the cell from Zn^{2+} cytotoxicity (Turney *et al.*, 2012; Vandebriel and De Jong, 2012; Bisht and Rayamajhi, 2016). All this evidence leads to the conclusion that the decrease in viability promoted by ZnO NPs at the tested concentrations and exposure times has a more toxic effect due to the dissolution of Zn^{2+} directly inside cells. The same is not true for $ZnSO_4$ because its Zn^{2+} cannot cross the membrane. So, 0.1 µg/mL ZnO concentration for incubation times shorter than 3hr does not reveal cell toxicity. This fact validates the possibility of using ZnO NPs in the research of protein expression changes, important for this study.

Subsequently, the effect of ZnO NPs interaction with some of the important proteins involved in the complex post-synaptic network showed important results of Zn^{2+} action, especially for PSD-95, SHANK 3 and β-actin levels. Although it is well known that the complex protein network in PSD plays a key role in the formation, maintenance, and connection of new cellular synapses and machinery within neuronal cells, little is known

about how this network interacts to make this happen. In fact, when 0.1 μg/mL ZnO NPs were used on SH-SY5Y cells, PSD-95 expression increased over time becoming significant after exposure times greater than 30 minutes. The same is not true when cells were subjected to 0.5 μg/mL ZnO NPs treatment. When the same treatment conditions are used to assess changes in SHANK 3 protein levels, a tendency to increase, although less pronounced and not significant, is recorded for 0.1 μg/mL treatment. A non-proportional reduction with time was observed in the case of 0.5 μg/mL ZnO NPs treatment. Finally, the results for β-actin are different from those obtained for PSD-95 and SHANK 3. They show no significant variations between the exposure times tested. Although a slight reduction between concentrations effect was also confirmed when the concentration of ZnO NPs increases from 0.1 μg/mL to 0.5 μg/mL. All this evidence leads to the conclusion that, in fact, Zn^{2+} of ZnO NPs at sub-toxicity concentrations may play an important role by increasing the levels of expression of PSD-95 and SHANK 3 proteins in the PSD complex.

ZnO NPs-dependent increase of the above-mentioned proteins may play an important role in the pathologies of some neurodegenerative diseases. In AD, due to the link between Aβ oligomers and NMDA, which in turn interacts with PSD-95, a direct relationship between Aβ oligomers and PSD-95 can occur (Dinamarca, Ríos and Inestrosa, 2012; Dinamarca *et al.*, 2015; Torres, Vallejo and Inestrosa, 2017). When cultured cortical neurons are exposed to Aβ oligomers a decrease in PSD-95 levels in time- and dose-dependent manner requiring NMDAR activation was observed (Lacor *et al.*, 2004; Roselli *et al.*, 2005). The same decrease was observed for SHANK 3 in human brain temporal lobe of AD patients. Thus, this reduction of PSD-95 and SHANK 3 compromises the synaptic plasticity responsible for the AD pathology. Results from mutant Htt in HD also improving synaptic proteins fold changes in human post-mortem brain in HD patients and animal model. Downregulated levels of PSD-95 were shown in striatum and barrel cortical neurons respectively. No information of SHANK 3 levels in neurons of HD patients is known (Fourie *et al.*, 2014; Smith *et al.*, 2014; Murmu *et al.*, 2015).

The association of the previously results with those obtained here allows us to speculate that the proposed model of the addition of ZnO NPs at sub-toxic concentrations may contribute to the increase of PSD-95 and SHANK 3 levels of relevance to neurodegenerative diseases. Thus, promising results may be visible in the formation of new altered excitatory

synapses in these diseases, contributing to the improvement of cognitive and motor functions. Clearly this needs to be further investigated.

7. Conclusions and future work

ZnO NPs plays an important role in cell viability and in sub-toxic concentration of 0.1 µg/mL, it can modulate specific post-synaptic proteins expression. Nevertheless, it is found that with increasing concentration of ZnO NPs exposure, the toxic effect increases. Moreover, the increase in ROS production, although not significant, is another fact that should be considered in future work. In summary, future investigations should be made to better characterize the toxic effect caused by increased ZnO NPs concentrations and increased ROS production. Imaging through fluorescence microscopy would be a relevant tool to verify changes in the mitochondria´s number and degeneration process after exposure to ZnO NPs treatment.

By comparing the effect of ZnO NPs with $ZnSO_4$ it is concluded that although $ZnSO_4$, according to the data, is less toxic to cells, more experiments should be performed. For this, it is proposed to perform an electroporation technique, through an electrical stimulus directly to the cells. Exposure to sufficiently intense stimulation will increase cell membrane permeability thereby reducing the barrier. This will facilitate the interaction of Zn^{2+} present in $ZnSO_4$ with the cellular components. Thus, the proposed conditions will be more similar to those obtained for the treatment of cells with ZnO NPs.

Finally, another parameter tested showed that ZnO NPs can be a fundamental mechanism in the synaptic modulation of altered synapses due to the increase of PSD-95 and SHANK 3 proteins levels.

Based on the results from this thesis a model in which the modulation of PSD-95 and SHANK 3 protein levels through sub-toxic ZnO NPS concentrations can act in signaling pathways altered in neurodegenerative diseases such AD and HD in proposed. The treatment may increase PSD-95 and SHANK 3 protein levels in PSD of cells from patients with these neurodegenerative diseases. This can contribute to the reduction of behaviour changes and to the correct function of new excitatory synapses. For this, it is important to differentiate SH-SY5Y cells to approximate the cell model used as closely as possible to the human neuronal model. Thus, more promising results from the impact of NPs on neuropathology-related proteins could be obtained. An immunocytochemistry method could be appropriate as a supplementary analysis of the data obtained so far and the proposed model. This technique through the specific antibodies could show how treatment impacts the levels of the proteins interest, by visualizing the distribution of target molecules. *In vivo*

assays could also be made through intravenous or nasal injection of ZnO NPs for further analysis.

The development of a new protein modulation mechanism through sub-toxic concentrations of ZnO NPs may represent an important step in neuroscience research through its contribution to the resolution or retardation of neurodegenerative diseases.

References

Andreini, C. *et al.* (2006) 'Counting the Zinc-Proteins Encoded in the Human Genome', *Journal of Proteome Research*, 5(1), pp. 196–201. doi: 10.1021/pr050361j.

Andreini, C., Bertini, I. and Cavallaro, G. (2011) 'Minimal Functional Sites Allow a Classification of Zinc Sites in Proteins', *PLoS ONE*. Edited by J. L. Sussman, 6(10), p. e26325. doi: 10.1371/journal.pone.0026325.

Arasu, M. V. *et al.* (2019) 'Synthesis and characterization of ZnO nanoflakes anchored carbon nanoplates for antioxidant and anticancer activity in MCF7 cell lines', *Materials Science and Engineering: C*, 102, pp. 536–540. doi: 10.1016/j.msec.2019.04.068.

Arons, M. H. et al. (2016) 'Shank3 is part of a zinc-sensitive signaling system that regulates excitatory synaptic strength', Journal of Neuroscience, 36(35), pp. 9124–9134. doi: 10.1523/JNEUROSCI.0116-16.2016.

Aydemir, T. B. et al. (2009) 'Zinc transporter ZIP8 (SLC39A8) and zinc influence IFN-gamma expression in activated human T cells.', Journal of leukocyte biology. The Society for Leukocyte Biology, 86(2), pp. 337–48. doi: 10.1189/jlb.1208759.

Bafaro, E. et al. (2017) 'The emerging role of zinc transporters in cellular homeostasis and cancer', Signal Transduction and Targeted Therapy, 2. doi: 10.1038/sigtrans.2017.29.

Barad, S. et al. (2017) 'Preparation and characterization of ZnO nanoparticles coated by chitosan-linoleic acid; fungal growth and biofilm assay', Bratislava Medical Journal, 118(03), pp. 169–174. doi: 10.4149/BLL_2017_034.

Baron, M. K. (2006) 'An Architectural Framework That May Lie at the Core of the Postsynaptic Density', *Science*, 311(5760), pp. 531–535. doi: 10.1126/science.1118995.

BartBomiej Pochwat, Gabriel Nowak, and B. S. (2015) 'Relationship between Zinc (Zn2+) and Glutamate Receptors in the Processes Underlying Neurodegeneration', *Neural Plasticity*, p. 9. Available at: http://downloads.hindawi.com/journals/np/2015/591563.pdf.

Bell, S. G. and Vallee, B. L. (2009) 'The Metallothionein/Thionein System: An Oxidoreductive Metabolic Zinc Link', *ChemBioChem*. John Wiley & Sons, Ltd, 10(1), pp. 55–62. doi: 10.1002/cbic.200800511.

Bio-Rad (2019) *Introduction to Western Blotting | Immunoblotting |*, *Bio-Rad*. Available at: https://www.bio-rad-antibodies.com/western-blotting-immunoblotting-introduction.html.

Biosciences, A. (1999) *Technical manual of Protein Electrophoresis - Chapter 1*.

Bisht, G. and Rayamajhi, S. (2016) 'ZnO Nanoparticles: A Promising Anticancer Agent', *SAGE Journal*, 3. doi: 10.5772/63437.

Blakemore, L. J. and Trombley, P. Q. (2004) 'Diverse modulation of olfactory bulb AMPA receptors by zinc', *NeuroReport*, 15(5), pp. 919–923. doi: 10.1097/00001756-200404090-00037.

Boeckers, T. M. *et al.* (1999) *Proline-Rich Synapse-Associated Protein-1/Cortactin Binding Protein 1 (ProSAP1/CortBP1) Is a PDZ-Domain Protein Highly Enriched in the Postsynaptic Density*. Available at: https://pdfs.semanticscholar.org/2fdb/179fc506c03047aac4edb721905f4e55e1d6.pdf.

Bogutska, K., Sklyarov, Y. and Prylutskyy, Y. (2013) 'Zinc and zinc nanoparticles: biological role and application in biomedicine', *Ukrainica bioorganica acta*, 1, pp. 9–16.

Bohic, S. *et al.* (2011) 'Biological roles of trace elements in the brain with special focus on Zn and Fe', *Revue Neurologique*. Elsevier Masson, 167(4), pp. 269–279. doi: 10.1016/J.NEUROL.2010.07.035.

Buse, J. and El-Aneed, A. (2010) 'Properties, engineering and applications of lipid-based nanoparticle drug-delivery systems: current research and advances', *Nanomedicine*, 5(8), pp. 1237–1260. doi: 10.2217/nnm.10.107.

Bush, A. I. and Tanzi, R. E. (2002) 'The galvanization of-amyloid in Alzheimer's disease', *PNAS*, 99(11), pp. 7317–7319. Available at: www.pnas.orgcgidoi10.1073pnas.122249699.

Canzoniero, L. M., Turetsky, D. M. and Choi, D. W. (1999) 'Measurement of intracellular free zinc concentrations accompanying zinc-induced neuronal death.', *The Journal of neuroscience : the official journal of the Society for Neuroscience*, 19(19). doi: 10.1523/jneurosci.19-19-j0005.1999.

Chen, L., Su, B. and Jiang, L. (2019) 'Recent advances in one-dimensional assembly of nanoparticles', *Chemical Society Reviews*. Royal Society of Chemistry, 48(1), pp. 8–21. doi: 10.1039/C8CS00703A.

Chhatre, A. *et al.* (2012) 'Color and surface plasmon effects in nanoparticle systems: Case of silver nanoparticles prepared by microemulsion route', *Colloids and Surfaces A: Physicochemical and Engineering Aspects*. Elsevier, 404, pp. 83–92. doi: 10.1016/J.COLSURFA.2012.04.016.

Craven, S. E. and Bredt, D. S. (1998) 'PDZ proteins organize synaptic signaling pathways', *Cell*, 93(4), pp. 495–498. doi: 10.1016/S0092-8674(00)81179-4.

Crews, L. and Masliah, E. (2010) ‘Molecular mechanisms of neurodegeneration in Alzheimer’s disease.’, *Human molecular genetics*. Oxford University Press, 19(R1), pp. R12-20. doi: 10.1093/hmg/ddq160.

Dan Guo et al (2014) ‘Mechanical properties of nanoparticles: basics and applications’, *Journal of Physics D: Applied Physics*, 47. doi: 10.1088/0022-3727/47/1/013001.

David D. Mott, M. B. and R. J. D. (2008) ‘pH-Dependent Inhibition of Kainate Receptors by Zinc’, *The Journal of Neuroscience*, 28, pp. 1659 –1671. Available at: http://europepmc.org/backend/ptpmcrender.fcgi?accid=PMC4100615&blobtype=pdf.

David L. BrautiganS, Paul Bornstein, and and Byron Gallis (1981) ‘Phosphotyrosyl-protein phosphatase. Specific inhibition by Zn.’, *The Journal of Cell Biology,* 256(No. 13), pp. 6519–6522. Available at: http://www.jbc.org/content/256/13/6519.full.pdf.

Díaz, M. and Vivas-Mejia, P. (2013) ‘Nanoparticles as Drug Delivery Systems in Cancer Medicine: Emphasis on RNAi-Containing Nanoliposomes’, *Pharmaceuticals*, 6(11), pp. 1361–1380. doi: 10.3390/ph6111361.

Dinamarca, M. C. *et al.* (2015) ‘The soluble extracellular fragment of neuroligin-1 targets Aβ oligomers to the postsynaptic region of excitatory synapses’, *Biochemical and Biophysical Research Communications*. Academic Press Inc., 466(1), pp. 66–71. doi: 10.1016/j.bbrc.2015.08.107.

Dinamarca, M. C., Ríos, J. A. and Inestrosa, N. C. (2012) ‘Postsynaptic receptors for amyloid-β oligomers as mediators of neuronal damage in Alzheimer’s disease’, *Frontiers in Physiology*. doi: 10.3389/fphys.2012.00464.

Dong, L. *et al.* (2019) ‘Shape-dependent toxicity of alumina nanoparticles in rat astrocytes’, *Science of The Total Environment*, 690, pp. 158–166. doi: 10.1016/j.scitotenv.2019.06.532.

Ebert, J. C. and Altman, R. B. (2008) 'Robust recognition of zinc binding sites in proteins', *The Protein Society*, 17(1), pp. 54–65. doi: 10.1110/ps.073138508.

Eide, D. J. (2006) 'Zinc transporters and the cellular trafficking of zinc', *Biochimica et Biophysica Acta (BBA) - Molecular Cell Research*, 1763(7), pp. 711–722. doi: 10.1016/j.bbamcr.2006.03.005.

Einav Cohen-Kfir, William Lee, Sepehr Eskandari, and N. N. (2005) 'Zinc inhibition of gamma-aminobutyric acid transporter 4. (GAT4) reveals a link between excitatory and inhibitory neurotransmission', *PNAS*, 102(No. 17), pp. 6154 – 6159. Available at: http://europepmc.org/backend/ptpmcrender.fcgi?accid=PMC556128&blobtype=pdf.

Eunjoon Kim and Morgan Sheng (2009) 'The postsynaptic density', *Cell Press*. Available at: https://www.cell.com/current-biology/pdf/S0960-9822(09)01473-0.pdf.

Fahrni, C. J. (2007) 'Biological applications of X-ray fluorescence microscopy: exploring the subcellular topography and speciation of transition metals', *Current Opinion in Chemical Biology*, 11(2), pp. 121–127. doi: 10.1016/j.cbpa.2007.02.039.

Fallis, A. . (2013) 'International Review of Neurobiology', *Journal of Chemical Information and Modeling*, 31(9), pp. 144–238. doi: 10.1017/CBO9781107415324.004.

Feng, W. *et al.* (2005) 'Metallothionein transfers zinc to mitochondrial aconitase through a direct interaction in mouse hearts', *Biochemical and Biophysical Research Communications*, 332(3), pp. 853–858. doi: 10.1016/j.bbrc.2005.04.170.

Firdos Alam Khan, Dana Almohazey, Munthar Alomari, S. A. A. (2018) 'Impact of nanoparticles on neuron biology: current research trends', *International Journal of Nanomedicine*, 13, pp. 2767–2776. Available at: https://www.ncbi.nlm.nih.gov/pmc/articles/PMC5951135/pdf/ijn-13-2767.pdf.

Fonseca-Santos, B. *et al.* (2015) 'Nanotechnology-based drug delivery systems for the treatment of Alzheimer's disease', *International Journal of Nanomedicine Dovepress*, 10, pp. 4981–5003. doi: 10.2147/IJN.S87148.

Fourie, C. *et al.* (2014) 'Differential Changes in Postsynaptic Density Proteins in Postmortem Huntington's Disease and Parkinson's Disease Human Brains', *Journal of Neuroscience diseases*. doi: 10.1155/2014/938530.

Frederickson, C. J. (1989) 'Neurobiology of Zinc and Zinc-Containing Neurons', in *Internation review of Neurobiology*, pp. 145–238. doi: 10.1016/S0074-7742(08)60279-2.

Frederickson, C. J., Koh, J.-Y. and Bush, A. I. (2005) 'The neurobiology of zinc in health and disease', *Nature Reviews Neuroscience*, 6(6), pp. 449–462. doi: 10.1038/nrn1671.

Fukada, T. *et al.* (2011) 'Zinc homeostasis and signaling in health and diseases', *JBIC Journal of Biological Inorganic Chemistry*, 16(7), pp. 1123–1134. doi: 10.1007/s00775-011-0797-4.

Fukada, T. and Kambe, T. (eds) (2014) *Zinc Signals in Cellular Functions and Disorders*. Tokyo: Springer Japan. doi: 10.1007/978-4-431-55114-0.

Futai, K. *et al.* (2007) 'Retrograde modulation of presynaptic release probability through signaling mediated by PSD-95–neuroligin', *Nature Neuroscience*, 10(2), pp. 186–195. doi: 10.1038/nn1837.

García-Pinel, B. *et al.* (2019) 'Lipid-based nanoparticles: Application and recent advances in cancer treatment', *Nanomaterials*, 9(4), pp. 1–23. doi: 10.3390/nano9040638.

Gawande, M. B. *et al.* (2015) 'Core–shell nanoparticles: synthesis and applications in catalysis and electrocatalysis', *Chemical Society Reviews*, 44(21), pp. 7540–7590. doi: 10.1039/C5CS00343A.

Genome Editing Proteins (2010) *Center for Biomolecular Modeling* . doi: 10.1146/annurev-biochem-010909-095056.

Ghasemi, A. *et al.* (2018) 'Optical Assays Based on Colloidal Inorganic Nanoparticles', *Analyst*, 143(14), pp. 3249–3283. doi: 10.1039/c8an00731d.

Ghassan, A., Mijan, N.-A. and Taufiq-Yap, Y. (2019) 'Nanomaterials: An Overview of Nanorods Synthesis and Optimization', in *Nanorods - An Overview from Synthesis to Emerging Device Applications*. doi: 10.5772/intechopen.84550.

Grabrucker, A. M. *et al.* (2009) 'Efficient targeting of proteins to post-synaptic densities of excitatory synapses using a novel pSDTarget vector system', *Journal of Neuroscience Methods*, 181(2), pp. 227–234. doi: 10.1016/j.jneumeth.2009.05.008.

Grabrucker, A. M. *et al.* (2011) 'Concerted action of zinc and ProSAP/Shank in synaptogenesis and synapse maturation', *EMBO Journal*. Nature Publishing Group, 30(3), pp. 569–581. doi: 10.1038/emboj.2010.336.

Gregori, M., Masserini, M. and Mancini, S. (2015) 'Nanomedicine for the treatment of Alzheimer's disease', *Nanomedicine*, 10(7), pp. 1203–1218. doi: 10.2217/nnm.14.206.

Guterres, S. S., Alves, M. P. and Pohlmann, A. R. (2007) 'Polymeric Nanoparticles, Nanospheres and Nanocapsules, for Cutaneous Applications', *Drug Target Insights*, 2, p. 117739280700200. doi: 10.1177/117739280700200002.

Halsted, J. A. (1961) 'Syndrome of iron deficiency Anemia, Hepatosplenomegaly, Hypogonadism, Dwarfism and Geophagia'. Am J Med 31, pp. 532–546. Available at: https://europepmc.org/backend/ptpmcrender.fcgi?accid=PMC2249139&blobtype=pdf.

Hancock', J. T., Desikan, R. and Neil, S. J. (2001) 'Role of reactive oxygen species in cell signalling pathways', *Biochemical Society transactions*, 2, pp. 345–50.

Hanley, C. *et al.* (2008) 'Preferential killing of cancer cells and activated human T cells using ZnO nanoparticles', *Nanotechnology*, 19(29), p. 295103. doi: 10.1088/0957-4484/19/29/295103.

Hansson, A. (1996) 'Extracellular Zinc Ions Induces Mitogen-Activated Protein Kinase Activity and Protein Tyrosine Phosphorylation in Bombesin-Sensitive Swiss 3T3 Fibroblasts', *Archives of Biochemistry and Biophysics*. Academic Press, 328(2), pp. 233–238. doi: 10.1006/ABBI.1996.0168.

Harish, K. K. *et al.* (2018) 'Metallic Nanoparticle: A Review', *Biomed J Sci &Tech Res*, 4(2). doi: 10.26717/BJSTR.2018.04.001011.

Hering, H. and Sheng, M. (2003) 'Activity-Dependent Redistribution and Essential Role of Cortactin in Dendritic Spine Morphogenesis', *The journal of neuroscience: the official journal of the Society for Neuroscience*, 23(37), p. 11759–69. Available at: https://www.jneurosci.org/content/jneuro/23/37/11759.full.pdf.

Huang, W. J., Chen, W. W. and Zhang, X. (2016) 'Huntington's disease: Molecular basis of pathology and status of current therapeutic approaches', *Experimental and Therapeutic Medicine*. Spandidos Publications, pp. 1951–1956. doi: 10.3892/etm.2016.3566.

Huang, Z. and Lippard, S. J. (2012) 'Illuminating mobile zinc with fluorescence: from cuvettes to live cells and tissues', in *Methods in Enzymology*. Cambridge, Massachusetts, USA, pp. 445–468. doi: 10.1016/B978-0-12-388448-0.00031-0.

Hui, A., Liu, J. and Ma, J. (2016) 'Synthesis and morphology-dependent antimicrobial activity of cerium doped flower-shaped ZnO crystallites under visible light irradiation', *Colloids and Surfaces A: Physicochemical and Engineering Aspects*, 506, pp. 519–525. doi: 10.1016/j.colsurfa.2016.07.016.

Hynd, M. R., Scott, H. L. and Dodd, P. R. (2004) 'Glutamate-mediated excitotoxicity and neurodegeneration in Alzheimer's disease', *Neurochemistry International*. Pergamon, 45(5), pp. 583–595. doi: 10.1016/J.NEUINT.2004.03.007.

Ilves, M. *et al.* (2014) 'Topically applied ZnO nanoparticles suppress allergen induced skin inflammation but induce vigorous IgE production in the atopic dermatitis mouse model', *Particle and Fibre Toxicology*, 11(1), p. 38. doi: 10.1186/s12989-014-0038-4.

Iravani, S. (2011) 'Green synthesis of metal nanoparticles using plants', *Green Chemistry*, 13(10), p. 2638. doi: 10.1039/c1gc15386b.

Jackson, M. J. (1989) 'Physiology of Zinc: General Aspects', in *Zinc in Human Biology*, pp. 1–14. doi: 10.1007/978-1-4471-3879-2_1.

Jennifer Gordon, Shohreh Amini, and M. K. W. (2014) 'General overview of neuronal cell culture', *Molecular Biology*, 1078, pp. 1–8. Available at: https://www.ncbi.nlm.nih.gov/pmc/articles/PMC4052554/pdf/nihms-587285.pdf.

Jesse L. Costales, A. K. (2015) 'Phelan–McDermid Syndrome and SHANK3: Implications for Treatment', *Neurotherapeutics*, 12, pp. 620–630. Available at: http://europepmc.org/backend/ptpmcrender.fcgi?accid=PMC4489957&blobtype=pdf.

Jiang, J., Pi, J. and Cai, J. (2018) 'The Advancing of Zinc Oxide Nanoparticles for Biomedical Applications', *Bioinorganic Chemistry and Applications*, 2018. doi: 10.1155/2018/1062562.

Jiang, Y. *et al.* (2016) 'Role of physical and chemical interactions in the antibacterial behavior of ZnO nanoparticles against E. coli', *Materials Science and Engineering C*. Elsevier Ltd, 69, pp. 1361–1366. doi: 10.1016/j.msec.2016.08.044.

K. Eric Drexler. (2006) *Engines of Creation: The Coming Era of Nanotechnology*. Available at: https://web.archive.org/web/20140810022659/http://www1.appstate.edu/dept/physics/nanotech/EnginesofCreation2_8803267.pdf.

Kambe, T. *et al.* (2015) 'The physiological, biochemical, and molecular roles of zinc transporters in zinc homeostasis and metabolism', *Physiological Reviews*, 95(3), pp. 749–784. doi: 10.1152/physrev.00035.2014.

Kambe, T., Tsuji, T. and Fukue, K. (2014) 'Zinc Transport Proteins and Zinc Signaling', in *Zinc Signals in Cellular Functions and Disorders*. Tokyo: Springer Japan, pp. 27–53. doi: 10.1007/978-4-431-55114-0_3.

Kestens Gert Roebben Jan Herrmann, V. A. *et al.* (2016) 'Challenges in the size analysis of a silica nanoparticle mixture as candidate certified reference material', *J Nanopart Res*, 18, p. 171. doi: 10.1007/s11051-016-3474-2.

Khan, I., Saeed, K. and Khan, I. (2017) 'Nanoparticles: Properties, applications and toxicities', *Arabian Journal of Chemistry*. Elsevier. doi: 10.1016/J.ARABJC.2017.05.011.

Kimura, T. and Kambe, T. (2016) 'The functions of metallothionein and ZIP and ZnT transporters: An overview and perspective', *International Journal of Molecular Sciences*, 17(3), pp. 10–12. doi: 10.3390/ijms17030336.

King, J. C., Shames, D. M. and Woodhouse, L. R. (2000) *Zinc homeostasis in humans.*, *J. Nutr*. Available at: https://academic.oup.com/jn/article-abstract/130/5/1360S/4686372.

Klug, A. (2010) 'The Discovery of Zinc Fingers and Their Applications in Gene Regulation and Genome Manipulation', *Annual Review of Biochemistry*, 79(1), pp. 213–231. doi: 10.1146/annurev-biochem-010909-095056.

Kluska, K., Adamczyk, J. and Krężel, A. (2018) 'Metal binding properties, stability and reactivity of zinc fingers', *Coordination Chemistry Reviews*. Elsevier, 367, pp. 18–64. doi: 10.1016/J.CCR.2018.04.009.

Kochańczyk, T., Drozd, A. and Krężel, A. (2015) 'Relationship between the architecture of zinc coordination and zinc binding affinity in proteins – insights into zinc regulation', *Metallomics*, 7(2), pp. 244–257. doi: 10.1039/C4MT00094C.

Korayem, A. H. *et al.* (2017) 'A review of dispersion of nanoparticles in cementitious matrices: Nanoparticle geometry perspective', *Construction and Building Materials*, 153, pp. 346–357. doi: 10.1016/j.conbuildmat.2017.06.164.

Kovalevich, J. and Langford, D. (2013) 'Considerations for the Use of SH-SY5Y Neuroblastoma Cells in Neurobiology', in, pp. 9–21. doi: 10.1007/978-1-62703-640-5_2.

Krężel, A., Hao, Q. and Maret, W. (2007) 'The zinc/thiolate redox biochemistry of metallothionein and the control of zinc ion fluctuations in cell signaling', *Archives of Biochemistry and Biophysics*, 463(2), pp. 188–200. doi: 10.1016/j.abb.2007.02.017.

Krężel, A. and Maret, W. (2006) 'Zinc-buffering capacity of a eukaryotic cell at physiological pZn', *JBIC Journal of Biological Inorganic Chemistry*, 11(8), pp. 1049–1062. doi: 10.1007/s00775-006-0150-5.

Krężel, A. and Maret, W. (2016) 'The biological inorganic chemistry of zinc ions', *Archives of Biochemistry and Biophysics*, 611, pp. 3–19. doi: 10.1016/j.abb.2016.04.010.

Król, A. *et al.* (2017) 'Zinc oxide nanoparticles: Synthesis, antiseptic activity and toxicity mechanism', *Advances in Colloid and Interface Science*, 249, pp. 37–52. doi: 10.1016/j.cis.2017.07.033.

Kumar, B. *et al.* (2017) 'Recent advances in nanoparticle-mediated drug delivery', *Journal of Drug Delivery Science and Technology*. Elsevier B.V., 41, pp. 260–268. doi: 10.1016/j.jddst.2017.07.019.

Kumar Sahu, M. (2019) *Semiconductor Nanoparticles Theory and Applications*, *International Journal of Applied Engineering Research*. Available at: http://www.ripublication.com.

Lacor, P. N. *et al.* (2004) 'Synaptic targeting by Alzheimer's-related amyloid β oligomers', *Journal of Neuroscience*, 24(45), pp. 10191–10200. doi: 10.1523/JNEUROSCI.3432-04.2004.

Larry Squire; Darwin Berg; Floyd Bloom; Sascha du Lac; Anirvan Ghosh; Nicholas Spitzer (2008) *FUNDAMENTAL NEUROSCIENCE THIRD EDITION*. Third. Edited by N. S. Larry Squire, Darwin Berg, Floyd Bloom, Sascha du Lac, Anirvan Ghosh. Available at: https://www.hse.ru/data/2013/10/09/1280379806/Fundamental Neuroscience (3rd edition) 2008.pdf.

Lee, J.-Y. *et al.* (2002) 'Contribution by synaptic zinc to the gender-disparate plaque formation in human Swedish mutant APP transgenic mice', *PNAS*, 99(11), pp. 7705–7710. Available at: www.pnas.orgcgidoi10.1073pnas.092034699.

Lin, J., Chen, X. and Huang, P. (2016) 'Graphene-Based Nanomaterials for Bioimaging Graphical abstract HHS Public Access', *Adv Drug Deliv Rev*, 105, pp. 242–254. doi: 10.1016/j.addr.2016.05.013.

Liu, J. *et al.* (2017) 'Zinc oxide nanoparticles induce toxic responses in human neuroblastoma SHSY5Y cells in a size-dependent manner', *International Journal of Nanomedicine*. Dove Press, Volume 12, pp. 8085–8099. doi: 10.2147/IJN.S149070.

Liuzzi, J. P. and Cousins, R. J. (2004) 'Mammalian and Zinc Transporters', *Annual Review of Nutrition*. Annual Reviews, 24(1), pp. 151–172. doi: 10.1146/annurev.nutr.24.012003.132402.

Lu, Q. *et al.* (2016) 'Intracellular zinc distribution in mitochondria, ER and the Golgi apparatus.', *International journal of physiology, pathophysiology and pharmacology*. e-Century Publishing Corporation, 8(1), pp. 35–43. Available at: http://www.ncbi.nlm.nih.gov/pubmed/27186321.

Maret, W. (2011) ‘Metals on the move: zinc ions in cellular regulation and in the coordination dynamics of zinc proteins’, *BioMetals*, 24(3), pp. 411–418. doi: 10.1007/s10534-010-9406-1.

Martínez-Carmona, M., Gun’Ko, Y. and Vallet-Regí, M. (2018) ‘Zno nanostructures for drug delivery and theranostic applications’, *Nanomaterials*, 8(4), pp. 1–27. doi: 10.3390/nano8040268.

Meyer Bodansky (1921) ‘The Zinc and Copper content of the human brain.’, *Journal of Biological Chemistry*, 48, pp. 361–364. doi: 10.18.

Meyer, G. *et al.* (2004) ‘The complexity of PDZ domain-mediated interactions at glutamatergic synapses: a case study on neuroligin’, *Neuropharmacology*, 47(5), pp. 724–733. doi: 10.1016/j.neuropharm.2004.06.023.

Mi, K. and Johnson, G. (2006) ‘The Role of Tau Phosphorylation in the Pathogenesis of Alzheimers Disease’, *Current Alzheimer Research*, 3(5), pp. 449–463. doi: 10.2174/156720506779025279.

Microscopy, F. and Cytometry, F. (2016) ‘Cellular ROS / Superoxide Detection Assay Kit Instructions for Use’, (May).

Miller, J., Mclachlan, A. D. and Klug, A. (1985) ‘Repetitive zinc-binding domains in the protein transcription factor LiA from Xenopus oocytes’, *EMBO Journal*, 4(6), pp. 1609–1614. Available at: http://europepmc.org/backend/ptpmcrender.fcgi?accid=PMC554390&blobtype=pdf.

Mireia Garriga-Canuta, Carmen Agustín-Pavóna, Frank Herrmanna,b, Aurora Sánchezd, Mara Dierssenb,c, Cristina Fillate, M. I. (2012) ‘Synthetic zinc finger repressors reduce mutant Huntingtin expression in the brain of R6/2 mice.’, *PNAS*, 109(45), pp. 3136–45. Available at: https://www.ncbi.nlm.nih.gov/pmc/articles/PMC3494930/pdf/pnas.201206506.pdf.

Mishra, P. K. *et al.* (2017) 'Zinc oxide nanoparticles: a promising nanomaterial for biomedical applications', *Drug Discovery Today*. Elsevier Ltd, 22(12), pp. 1825–1834. doi: 10.1016/j.drudis.2017.08.006.

Molnár, P. and Nadler, J. V. (2001) 'Synaptically-released zinc inhibits N-methyl-d-aspartate receptor activation at recurrent mossy fiber synapses', *Brain Research*, 910(1–2), pp. 205–207. doi: 10.1016/S0006-8993(01)02720-2.

Moreno-Vega, A.-I. *et al.* (2012) 'Polymeric and Ceramic Nanoparticles in Biomedical Applications', *Journal of Nanotechnology*. Hindawi Publishing Corporation, pp. 1–10. doi: 10.1155/2012/936041.

Morgan Sheng and Eunjoon Kim (2000) 'Shank family of scaffold proteins', *Journal of Cell Science*, 113, pp. 1851–1856. Available at: https://pdfs.semanticscholar.org/66d0/25c05ebb5074ca89923194c15f95d7175549.pdf.

Murmu, R. P. *et al.* (2015) 'Altered sensory experience exacerbates stable dendritic spine and synapse loss in a mouse model of huntington's disease', *Journal of Neuroscience*. Society for Neuroscience, 35(1), pp. 287–298. doi: 10.1523/JNEUROSCI.0244-14.2015.

Murphy, B. C. J. and Jana, N. R. (2002) 'Controlling the Aspect Ratio of InorganicNanorods and Nanowires', in *Advanced Materials*, pp. 80–82.

Naisbitt, S. *et al.* (1999) 'Shank, a novel family of postsynaptic density proteins that binds to the NMDA receptor/PSD-95/GKAP complex and cortactin', *Neuron*, 23(3), pp. 569–582. doi: 10.1016/S0896-6273(00)80809-0.

Nazarizadeh, A. and Asri-Rezaie, S. (2016) 'Comparative Study of Antidiabetic Activity and Oxidative Stress Induced by Zinc Oxide Nanoparticles and Zinc Sulfate in Diabetic Rats', *AAPS PharmSciTech*. AAPS PharmSciTech, 17(4), pp. 834–843. doi: 10.1208/s12249-015-0405-y.

Neeran Obied Jasim (2015) 'Antifungal Activity of Zinc Oxide Nanoparticles on Aspergillus Fumigatus Fungus & amp;Candida Albicans Yeast', *Journal of Natural Sciences Research*, 5(4), pp. 2224–3186. Available at: http://citeseerx.ist.psu.edu/viewdoc/download?doi=10.1.1.1022.912&rep=rep1&type=pdf.

P. Coyle, J. C. Philcoxa, L. C. Careya, A. M. R. (2002) 'Metallothionein: the multipurpose protein.', *Cellular and Molecular Life Sciences*, 59, pp. 627–647. Available at: https://link.springer.com/content/pdf/10.1007%2Fs00018-002-8454-2.pdf.

Pal, S. L. *et al.* (2011) 'Nanoparticle: An overview of preparation and characterization', *Journal of applied pharmaceutical Science*, 01(06), pp. 228–234.

Paoletti, P. *et al.* (2000) 'Molecular Organization of a Zinc Binding N-Terminal Modulatory Domain in a NMDA Receptor Subunit', *Neuron*. Cell Press, 28(3), pp. 911–925. doi: 10.1016/S0896-6273(00)00163-X.

Paoletti, P. *et al.* (2009) 'Zinc at glutamatergic synapses', *Neuroscience*. Pergamon, 158(1), pp. 126–136. doi: 10.1016/J.NEUROSCIENCE.2008.01.061.

Pavlica, S., Gaunitz, F. and Gebhardt, R. (2009) 'Comparative in vitro toxicity of seven zinc-salts towards neuronal PC12 cells', *Toxicology in Vitro*, 23(4), pp. 653–659. doi: 10.1016/j.tiv.2009.03.003.

Pavlica, S. and Gebhardt, R. (2010) 'Comparison of uptake and neuroprotective potential of seven zinc-salts', *Neurochemistry International*, 56(1), pp. 84–93. doi: 10.1016/j.neuint.2009.09.005.

Petralia, R. S., Al-Hallaq, R. A. and Wenthold, R. J. (2008) 'Trafficking and targeting of NMDA receptors', in *Biology of the NMDA Receptor*. CRC Press, pp. 149–200. doi: 10.1201/9781420044157.ch8.

Pezeshki-Nejad, Z. *et al.* (2019) 'Tunable optical, electronic and magnetic properties of semiconductor nanoparticles induced by magnetic and nonmagnetic dopants: A comparative experimental and theoretical study', *Ceramics International*, 45(6), pp. 6912–6924. doi: 10.1016/j.ceramint.2018.12.188.

Pivovarova, N. B. *et al.* (2014) 'The interactive roles of zinc and calcium in mitochondrial dysfunction and neurodegeneration', *Journal of Neurochemistry*, 128(4), pp. 592–602. doi: 10.1111/jnc.12489.

Portbury, S. D. and Adlard, P. A. (2017) 'Zinc Signal in Brain Diseases', *Internation Journal of Molecular Sciences*, 18, pp. 1–13. doi: 10.3390/ijms18122506.

Purves D., G. J. A. (2015) *Neuroscience, 5rd Edition*.

Qiao, W. *et al.* (2006) 'Zinc binding to a regulatory zinc-sensing domain monitored in vivo by using FRET', *Proceedings of the National Academy of Sciences*, 103(23), pp. 8674–8679. doi: 10.1073/pnas.0600928103.

Qin, Y. *et al.* (2011) 'Measuring steady-state and dynamic endoplasmic reticulum and Golgi Zn 2þ with genetically encoded sensors', *Proceedings of the National Academy of Sciences of the United States of America*, 108(18), p. 5. doi: 10.1073/pnas.1015686108/-/DCSupplemental.

Qin, Z. *et al.* (2011) 'Trace metal imaging with high spatial resolution: Applications in biomedicine', *Metallomics*, 3(1), pp. 28–37. doi: 10.1039/C0MT00048E.

Qualmann, B. *et al.* (2004) 'Linkage of the Actin Cytoskeleton to the Postsynaptic Density via Direct Interactions of Abp1 with the ProSAP/ Shank Family', *The Journal of neuroscience : the official journal of the Society for Neuroscience*, 24(10), pp. 2481–95. doi: 10.1523/JNEUROSCI.5479-03.2004.

R, A. Mk. (2018) ‘Morphological and Biochemical Features of Cerebellar Cortex After Exposure to Zinc Oxide Nanoparticles : Possible Protective Role of Curcumin’, *Biology, Cell*, 301(8), pp. 1454–1466. doi: 10.1002/ar.23807.

Rasmussen, J. W. *et al.* (2010) ‘Zinc oxide nanoparticles for selective destruction of tumor cells and potential for drug delivery applications’, *Expert Opinion on Drug Delivery*, pp. 1063–1077. doi: 10.1517/17425247.2010.502560.

Raulin J., H. M.-E. (1869) *Annales Des Sciences Naturelles*, *Vol. 11*. Available at: https://sites.google.com/site/fednuckbackpont/home/annales-des-s-ywpgsfqg7py6tu.

Reyes, J. G. (1996) ‘Zinc transport in mammalian cells’, *American Journal of Physiology - Cell Physiology*, 270(2 39-2). doi: 10.1152/ajpcell.1996.270.2.C401.

Robert J. Cousins1 and Juan P. Liuzzi, and L. A. L. (2006) ‘Mammalian zinc transport, trafficking, and signals’, *THE JOURNAL OF BIOLOGICAL CHEMISTRY*, 281(No. 34), pp. 24085–24089. Available at: http://www.jbc.org/content/281/34/24085.full.pdf.

Romorini, S. *et al.* (2004) ‘A Functional Role of Postsynaptic Density-95-Guanylate Kinase-Associated Protein Complex in Regulating Shank Assembly and Stability to Synapses’, *The Journal of neuroscience : the official journal of the Society for Neuroscienceournal of Neuroscience*, 24(42), pp. 9391–404. doi: 10.1523/JNEUROSCI.3314-04.2004.

Roselli, F. *et al.* (2005) ‘Soluble β-amyloid1-40 induces NMDA-Dependent Degradation of Postsynaptic Density-95 at Glutamatergic Synapses’, *Journal of Neuroscience*, 25(48), pp. 11061–11070. doi: 10.1523/JNEUROSCI.3034-05.2005.

Rost, E. (1920) ‘Zinc and copper, regular constituents of the human body’, *Journal of the Franklin Institute*. Elsevier BV, 190(1), p. 153. doi: 10.1016/s0016-0032(20)92164-6.

Roussignol, G. *et al.* (2005) 'Shank Expression Is Sufficient to Induce Functional Dendritic Spine Synapses in Aspiny Neurons', 25(14), pp. 3560–70. doi: 10.1523/JNEUROSCI.4354-04.2005.

S. V. Razin, V. V. Borunova, O. G. M. and O. L. K. (2012) 'Cys2His2 Zinc Finger Protein Family: Classification, Functions, and Major Members', *Biokhimiya*, 77(No. 3), pp. 277–288. Available at: https://link.springer.com/content/pdf/10.1134%2FS0006297912030017.pdf.

Sala, C. *et al.* (2001) 'Regulation of Dendritic Spine Morphology and Synaptic Function by Shank and Homer', *Neuron*. Cell Press, 31(1), pp. 115–130. doi: 10.1016/S0896-6273(01)00339-7.

Sala, C. *et al.* (2005) 'Key Role of the Postsynaptic Density Scaffold Proteins Shank and Homer in the Functional Architecture of Ca 2 Homeostasis at Dendritic Spines in Hippocampal Neurons', *The Journal of neuroscience : the official journal of the Society for Neuroscience*, 25(18), pp. 4587–92. doi: 10.1523/JNEUROSCI.4822-04.2005.

Salahuddin Siddiqi, K., ur Rahman, A. and Husen, A. (2018) 'Properties of Zinc Oxide Nanoparticles and Their Activity Against Microbes', *Nanoscale Research Letters*, 13(141). doi: 10.1186/s11671-018-2532-3.

Salata, O. (2004) 'Applications of nanoparticles in biology and medicine', *Journal of Nanobiotechnology*. BioMed Central, 2(1), p. 3. doi: 10.1186/1477-3155-2-3.

Satoru Yamasaki, Kumiko Sakata-Sogawa, Aiko Hasegawa, Tomoyuki Suzuki, K. K., Emi Sato, Tomohiro Kurosaki, Susumu Yamashita, Makio Tokunaga, K. N. and T. and Hirano (2007) 'Zinc Is a Novel Intracellular Second Messenger', *The Journal of Cell Biology,* 177(No. 4), pp. 637–645. Available at: https://sci-hub.tw/10.2307/30052034.

Scheuing, L. *et al.* (2014) 'Preclinical and clinical investigations of mood stabilizers for Huntington's disease: What have we learned?', *International Journal of Biological Sciences*. Ivyspring International Publisher, 10(9), pp. 1021–1038. doi: 10.7150/ijbs.9898.

Schulz, M. J. *et al.* (2014) 'New Applications and Techniques for Nanotube Superfiber Development', in *Nanotube Superfiber Materials*. Elsevier, pp. 33–59. doi: 10.1016/B978-1-4557-7863-8.00002-5.

Science Photo Library (no date) *Zinc, atomic structure*. Available at: https://www.sciencephoto.com/media/460731/view/zinc-atomic-structure.

Scott, D. A. and Fisher, A. M. (1938) *The insulin and the Zinc content of normal and diabetic pancreas*. Available at: http://europepmc.org/backend/ptpmcrender.fcgi?accid=PMC434829&blobtype=pdf.

Segal, D. *et al.* (2004) 'A role for ZnT-1 in regulating cellular cation influx', *Biochemical and Biophysical Research Communications*, 323(4), pp. 1145–1150. doi: 10.1016/j.bbrc.2004.08.211.

Shabb, J. B., Muhonen, W. W. and Mehus, A. A. (2017) 'Quantitation of Human Metallothionein Isoforms in Cells, Tissues, and Cerebrospinal Fluid by Mass Spectrometry', *Methods in Enzymology*. Academic Press, 586, pp. 413–431. doi: 10.1016/BS.MIE.2016.11.004.

Shim, K. H. *et al.* (2014) 'Assessment of ZnO and SiO2 nanoparticle permeability through and toxicity to the blood–brain barrier using evans blue and tem', *International Journal of Nanomedicine*, 9, pp. 225–233. doi: 10.2147/IJN.S58205.

Sindreu, C. and Storm, D. R. (2011) 'Modulation of neuronal signal transduction and memory formation by synaptic zinc', *Frontiers in Behavioral Neuroscience*, 5(68). doi: 10.3389/fnbeh.2011.00068.

Smith, G. A. *et al.* (2014) 'Progressive axonal transport and synaptic protein changes correlate with behavioral and neuropathological abnormalities in the heterozygous Q175 KI mouse model of Huntington's disease', *Human Molecular Genetics*. Oxford University Press, 23(17), pp. 4510–4527. doi: 10.1093/hmg/ddu166.

Smith, M. A. (1998) 'Alzheimer Disease', *International Review of Neurobiology*. Academic Press, 42, pp. 1–54. doi: 10.1016/S0074-7742(08)60607-8.

Soltau, M. *et al.* (2004) 'Insulin receptor substrate of 53kDa links postsynaptic shank to PSD-95', *Journal of Neurochemistry*, 90(3), pp. 659–665. doi: 10.1111/j.1471-4159.2004.02523.x.

Stoltenberg, M. *et al.* (2007) 'Amyloid plaques arise from zinc-enriched cortical layers in APP/PS1 transgenic mice and are paradoxically enlarged with dietary zinc deficiency', *Neuroscience*, 150(2), pp. 357–369. doi: 10.1016/j.neuroscience.2007.09.025.

Sun, Q., Li, J. and Le, T. (2018) 'Zinc Oxide Nanoparticle as a Novel Class of Antifungal Agents: Current Advances and Future Perspectives', *Journal of Agricultural and Food Chemistry*, 66(43), pp. 11209–11220. doi: 10.1021/acs.jafc.8b03210.

Takafumi Hara, Taka-aki Takeda, Teruhisa Takagishi, Kazuhisa Fukue, Taiho Kambe, T. F. (2017) 'Physiological roles of zinc transporters: molecular and genetic importance in zinc homeostasis', *J Physiol Sci*, 67, pp. 283–301. Available at: https://jps.biomedcentral.com/track/pdf/10.1007/s12576-017-0521-4.

Takagishi, T., Hara, T. and Fukada, T. (2017) 'Recent Advances in the Role of SLC39A/ZIP Zinc Transporters In Vivo', *International journal of molecular sciences*, 18(12). doi: 10.3390/ijms18122708.

Tao-Cheng, J.-H. *et al.* (2015) 'Differential Distribution of Shank and GKAP at the Postsynaptic Density', *PLoS ONE*, 10(3), p. 3. doi: 10.1371/journal.pone.0118750.

Tao-Cheng, J. H. *et al.* (2016) 'Zinc Stabilizes Shank3 at the Postsynaptic Density of Hippocampal Synapses', *PloS one*, 11(5), p. e0153979. doi: 10.1371/journal.pone.0153979.

Therapeutics, S. (2019) 'The activity of disease allele-selective zinc finger proteins in preclinical models of Huntington ' s disease', *Genomic medicine company*, (July), pp. 2–4.

Thiers, R. E. and Vallee, B. L. (1957) 'Distribution of metals in subcellular fractions of rat liver.', *The Journal of biological chemistry*, 226(2), pp. 911–920. Available at: http://www.jbc.org/.

Thomas, S. *et al.* (2015) 'Ceramic Nanoparticles: Fabrication Methods and Applications in Drug Delivery', *Current Pharmaceutical Design*, 21(42), pp. 6165–6188. doi: 10.2174/1381612821666151027153246.

Tian, L. *et al.* (2015) 'Neurotoxicity induced by zinc oxide nanoparticles: Age-related differences and interaction', *Scientific Reports*. Nature Publishing Group, 5. doi: 10.1038/srep16117.

Tiwari, J. N., Tiwari, R. N. and Kim, K. S. (2012) 'Zero-dimensional, one-dimensional, two-dimensional and three-dimensional nanostructured materials for advanced electrochemical energy devices', *Progress in Materials Science*, 57(4), pp. 724–803. doi: 10.1016/j.pmatsci.2011.08.003.

Torres, V. I., Vallejo, D. and Inestrosa, N. C. (2017) 'Emerging Synaptic Molecules as Candidates in the Etiology of Neurological Disorders', *Neural Plasticity*. doi: 10.1155/2017/8081758.

Turney, T. W. *et al.* (2012) 'Formation of zinc-containing nanoparticles from Zn2+ ions in cell culture media: Implications for the nanotoxicology of ZnO', *Chemical Research in Toxicology*, 25(10), pp. 2057–2066. doi: 10.1021/tx300241q.

Umrani, R. D. and Paknikar, K. M. (2014) 'Zinc oxide nanoparticles show antidiabetic activity in streptozotocin- induced Type 1 and 2 diabetic rats', *Nanomedicine*. Future Medicine Ltd., 9(1), pp. 89–104. doi: 10.2217/nnm.12.205.

Valdiglesias, V. *et al.* (2013) 'Neuronal cytotoxicity and genotoxicity induced by zinc oxide nanoparticles', *Environment International*. Elsevier Ltd, 55, pp. 92–100. doi: 10.1016/j.envint.2013.02.013.

Vandebriel, R. J. and De Jong, W. H. (2012) 'A review on mammalian toxicity of zno nanoparticles ', *Science and Applications*, 5, pp. 61–71. doi: 10.2147/NSA.S23932.

Verena von Bülow, L. R. and H. H. (2005) 'Zinc-mediated inhibition of cyclic nucleotide phosphodiesterase activity and expression suppresses TNF-alpha and IL-1 beta production in monocytes by elevation of guanosine 3=,5=-cyclic monophosphate', 175, pp. 4697–4705. Available at: https://www.jimmunol.org/content/jimmunol/175/7/4697.full.pdf.

Verpelli, C. *et al.* (2012) 'Scaffold Proteins at the Postsynaptic Density', *Advances in Experimental Medicine and Biology*, 970. doi: 10.1007/978-3-7091-0932-8_2.

Vijay Kumar, Ashok Kumar,Sandeep Kumar Singh, Sanjeev Kumar, T. *et al.* (2016) 'Zinc Deficiency and Its Effect on the Brain: An Update', *International Journal of Molecular Genetics and Gene Therapy*, 1.1, pp. 2471–4968. Available at: https://www.sciforschenonline.org/journals/genetics/article-data/SGGT-1-105/SGGT-1-105.pdf.

Wang, Y. and Xia, Y. (2004) 'Bottom-Up and Top-Down Approaches to the Synthesis of Monodispersed Spherical Colloids of Low Melting-Point Metals', *Nano Letters*, 4(10), pp. 2047–2050. doi: 10.1021/nl048689j.

Webster, T. J. (2008) 'Decreased astroglial cell adhesion and proliferation on zinc oxide nanoparticle polyurethane composites', *International Journal of Nanomedicine*, p. 523. doi: 10.2147/IJN.S4346.

Weeks, M. E. (1932) ‘The discovery of the elements. III. Some eighteenth-century metals’, *J. Chem. Educ.*, 9(1), p. 22. doi: 10.1021/ed009p22.

Wolfgang Maret (2013) ‘Zinc Biochemistry: From a Single Zinc Enzyme to a Key Element of Life’, *American Society for Nutrition*, 4, pp. 82–91. Available at: https://watermark.silverchair.com/82.pdf.

Wu, A. R. and Yu, L. (2017) ‘There’s plenty of room at the bottom of a cell’, *Chemical Engineering Progress*, 113(10). Available at: http://nanoparticles.org/pdf/Feynman.pdf.

Yan, Q.-L. *et al.* (2016) ‘Highly energetic compositions based on functionalized carbon nanomaterials’, *Nanoscale*, 8(9), pp. 4799–4851. doi: 10.1039/C5NR07855E.

Yin, S. (2017) ‘Zinc oxide nanoparticles induce toxic responses in human neuroblastoma SHSY5Y cells in a size- dependent manner’, pp. 8085–8099.

Zhang, Y. *et al.* (2013) ‘Biomedical Applications of Zinc Oxide Nanomaterials’, *Current Molecular Medicine*, 13(10), pp. 1633–1645. doi: 10.2174/15665240136661311111130058.

A.Supplementary tables

Supplementary table 1- Zinc transporters (ZnTs) localization and corresponding transport function.

Families of Zn Transport proteins	Family member	Transport expression	Subcelullar localization
ZnTs	**ZnT1**	Export cytosolic Zn into the extracellular space;	Plasma membrane, basolateral membrane of polarized epithelial cells and apical membrane in pancreatic acinar cells
	ZnT2	Transport surplus cytosolic Zn into the lumen of vesicular compartments;	Ensosomes, lysosomes, endoplasmatic reticulum, inner mitochondrial membrane of mammalian cells
	ZnT3	Transport Zn into synaptic vesicles of a subset of glutaminergic neurons in the hippocampus and neocortex;	Synaptic vesicles
	ZnT4	Maintenance of cytosolic zinc homeostasis by controlling Zn translocation to the organelles;	Endossomes, lysosomes, cytoplamatic vesicles, golgi apparatus, trans-Golgi network (TGN)
	ZnT5	Supply Zn into the lumen during zinc deficiency, which induces the unfolded protein response (UPR).	Early secretory pathways (COPII coated vesicles and Golgi apparatus).
	ZnT6	Modulator subunit of Zn transport activity of ZnT5-ZnT6 heterodimers;	Golgi apparatus and TGN
	ZnT7	Active alkaline phosphatase (ALP) and contributes to homeostatic concentration in the early secretory pathway in cooperation with ZnT5-ZnT6 heterodimers.	Golgi apparatus
	ZnT8	Enhances glucose-stimulated insulin secretion in a high glucose challenge;	Pancreatic β-cell
	ZnT9	Nuclear receptor activator;	Cytoplasm
	ZnT10	Manganese transport.	Early/ recycling endosomes, Golgi apparatus

Supplementary table 2 - Zinc- and iron-like regulatory proteins (ZIPs) localization and corresponding transport function.

Families of Zn Transport proteins	Family member	Transport expression	Subcelullar localization
ZIPs	**ZIP1**	Export cytosolic Zn into the extracellular space;	Plasma membrane, basolateral membrane of polarized epithelial cells and apical membrane in pancreatic acinar cells
	ZIP2	Transport surplus cytosolic Zn into the lumen of vesicular compartments;	Endosomes, lysosomes, ER and inner mitochondrial membrane of mammalian cells
	ZIP3	Imports zinc from the extracellular space	Plasma membrane and apical membrane
	ZIP4	essential in dietary zinc absorption in mammals and role in intestinal integrity	Apical membrane of Duodenum and Jejunum.
	ZIP5	Functional as a zinc importer and participation in the control of zinc excretion.	Basolateral membrane of polarized cells
	ZIP6	Molecule through which zinc influx functions from the extracellular space	Plasma membrane
	ZIP 7	regulating LPS-induced cell surface MHC class II expression or tuning the TCR activation threshold in T cells which contributes to dendritic cell maturation negatively and possible role in immune functions; Regulation of zinc release from the intracellular stores which promotes activation of tyrosine kinases, AKT and ERKs, both involved in regulating cell proliferation and migration;	ER and Golgi apparatus
	ZIP 8	Increases the cytosolic zinc status and play pivotal roles in a negative-feedback loop that directly regulates the innate immune function	Plasma membrane, and apical surface of polarized cells and lysosome
	ZIP 9	Crucial role in B-cell receptor (BCR) signalling through regulation of Akt and ERK activity by translocate zinc from the Golgi lumen	Golgi apparatus and the cell surface
	ZIP10	Cell surface zinc importer indispensable for B-cell development in early and mature stages	Apical membrane
	ZIP11	Physiological and cellular functions have not been well defined.	Nucleus or Golgi apparatus
	ZIP12	Imports extracellular zinc into the cytosol facilitating zinc uptake into the cytosol, which mediates CREB activation via phosphorylation contributing for neuronal differentiation	Plasma membrane
	ZIP13	Mobilizes zinc from the lumen of organelles and plays pivotal roles in cellular signalling regulating the nuclear translocation of Smad proteins and in ER homeostatic maintenance	Golgi apparatus and cytoplasmic vesicles
	ZIP14	Import zinc, it is important to regulate systemic growth and it can mobilize various divalent cations, including iron, manganese, and cadmium	Plasma membrane, apical surface localization in polarized cells

Supplementary table 2 - Morphologies types of nanoparticles and respective functions and characteristics. Adapted from (Guterres, Alves and Pohlmann, 2007; Pal *et al.*, 2011; Schulz *et al.*, 2014; Fonseca-Santos *et al.*, 2015; Dong *et al.*, 2019; Ghassan, Mijan and Taufiq-Yap, 2019).

Nanoparticle morphology type	Principal Characteristics	Applications
Quantum dots (QDs)	Smallest devices containing a tiny droplet of free electrons; Colloidal semiconductor nanocrystals with range from 2 to 10 nm in diameter; Colloidal synthesis or electrochemistry	Optical and optoelectronic devices; Quantum computing; Information storage.
Nanotubes	Synthesis, properties and performance are dependent of number of walls, length, chirality, van der Waals forces, and quality with high impact in composition and geometry of these materials;	Neural scaffolds; Neurite regeneration; Replace metal wire for crossing the skin.
Nanospheres	Compose colloidal systems with aqueous cores; Responsible for assembly therapeutic agents within a colloidal matrix or can be attached to the particle surface by adsorption or conjugation processes; synthetized by polymeric membrane materials such (poly (butyl cyanoacrylate) (PBCA), poly (lactic acid) (PLA) or its copolymer poly(lactide-co-glycolide) (PLGA), alginate, chitosan, and other polymer combinations;	Drive the drug by entrapment, dispersion, dissolution within or adsorb
Nanowires	Thin wire; Diameter less than or equal to 100 nm; Synthesis made from a wide variety of materials, including silicon, germanium, carbon, and various conductive metals, such as gold and copper;	Replacement or repair of dysfunctional proteins due to your ability to create artificial protein-coding DNA.
Nanorods	Typical lengths of 10–120 nm; Synthesis made from metals, semiconductor, carbon, and oxides materials.	Development of electronic, optical, magnetic, and micromechanical devices

Supplementary table 3 - Resolution gel composition

Components of the resolution gel (1 system - 1.5mm)	5%	7.5%	8.5%	10%	20%
ddH2O (mL)	18.59	33.42	15.96	29.67	7.34
Bis/Acrylamide (mL)	3.75	11.25	6.38	15	15
LGB (mL)	7.5	15	7.5	15	7.5
APS (µL)	150	300	150	300	150
TEMED (µL)	15	30	15	30	15

Supplementary table 4 - Packaging gel composition

Packaging gel components (3.5 % acrylamide – 1.5 mm)	½ system	1 system
ddH2O (mL)	6.92	13.83
Bis/Acrylamide (mL)	0.88	1.75
UGB (mL)	2	4
SDS (µL)	100	200
APS (µL)	100	200
TEMED (µL)	10	20

Supplementary table 5 - Loading buffer composition

Loading Buffer Composition Reagent	Quantity
Tris-HCl (pH = 6.8) (mL)	2.5
SDS (g)	0.8
Bromophenol blue (mg)	1
Glycerol (mL)	4
β-Mercaptoethanol (mL)	2

Supplementary table 6 - Transfer buffer composition

Transfer Buffer Composition 5x:	V= 1 L	V= 2 L	V= 4 L
Tris (g)	15.15	30.30	60.60
Glycine (g)	72.05	144.1	288.2

Supplementary table 7 – TBS buffer composition

TBS Buffer Composition 5x:	V= 0.5 L	V= 1 L
Tris (g)	6.055	12.11
NaCl (g)	43.83	87.66

B. Supplementary figures

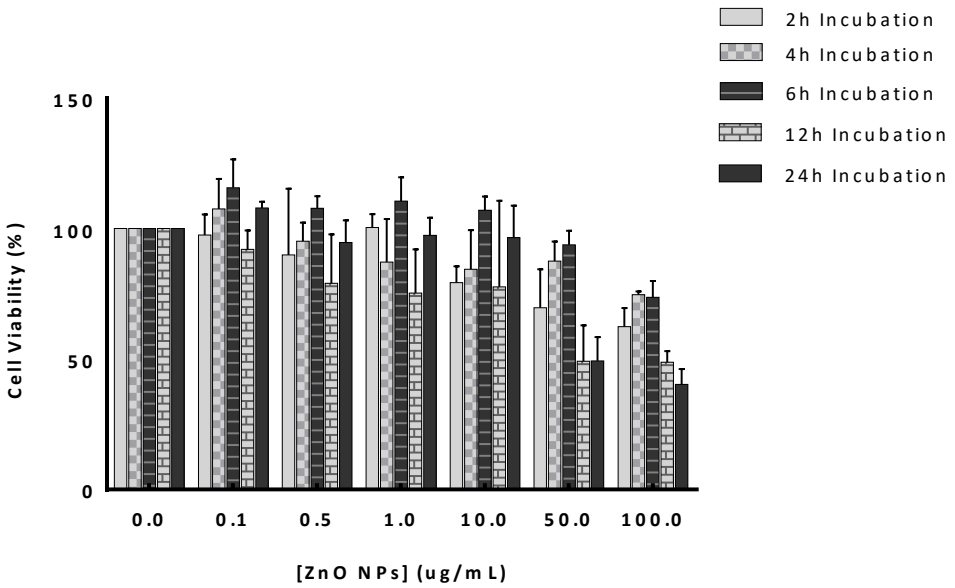

Supplementary figure 2 - Overall effects of ZnO NPs on SH-SY5Y cells' viability. Percentage of SH-SY5Y viability was measure for different concentrations (0.0, 0.1, 0.5, 10.0, 50.0 and 100.0 µg/mL) and timepoints (2, 4, 6, 12 and 24 hr) conditions, using a resazurin solution after cells exposure to each ZnO NPs concentration during the different exposure times. Cell viability was expressed as a function of control, where control was a set as 100%.Graph bars correspond to the mean of viable cells percentage for each ZnO NPs concentration tested with the respective SEM. Results are represent as a fold change over control. P values is <0,05, ns, non-significate, N=12.